INTERNATIONAL JOURNAL OF

BIOMETRICS AND BIOINFORMATICS (IJBB)

INTERNATIONAL JOURNAL OF BIOMETRICS AND BIOINFORMATICS (IJBB)

VOLUME 6, ISSUE 1, 2012

EDITED BY
DR. NABEEL TAHIR

INTERNATIONAL JOURNAL OF BIOMETRICS AND BIOINFORMATICS (IJBB)

CSC Publishers, 2012

EDITORIAL PREFACE

This is the first issue of volume six of International Journal of Biometric and Bioinformatics (IJBB). The Journal is published bi-monthly, with papers being peer reviewed to high international standards. The International Journal of Biometric and Bioinformatics is not limited to a specific aspect of Biology but it is devoted to the publication of high quality papers on all division of Bio in general. IJBB intends to disseminate knowledge in the various disciplines of the Biometric field from theoretical, practical and analytical research to physical implications and theoretical or quantitative discussion intended for academic and industrial progress. In order to position IJBB as one of the good journal on Bio-sciences, a group of highly valuable scholars are serving on the editorial board. The International Editorial Board ensures that significant developments in Biometrics from around the world are reflected in the Journal. Some important topics covers by journal are Bio-grid, biomedical image processing (fusion), Computational structural biology, Molecular sequence analysis, Genetic algorithms etc.

The initial efforts helped to shape the editorial policy and to sharpen the focus of the journal. Starting with volume 6, 2012, IJBB appears in more focused issues. Besides normal publications, IJBB intend to organized special issues on more focused topics. Each special issue will have a designated editor (editors) – either member of the editorial board or another recognized specialist in the respective field.

The coverage of the journal includes all new theoretical and experimental findings in the fields of Biometrics which enhance the knowledge of scientist, industrials, researchers and all those persons who are coupled with Bioscience field. IJBB objective is to publish articles that are not only technically proficient but also contains information and ideas of fresh interest for International readership. IJBB aims to handle submissions courteously and promptly. IJBB objectives are to promote and extend the use of all methods in the principal disciplines of Bioscience.

IJBB editors understand that how much it is important for authors and researchers to have their work published with a minimum delay after submission of their papers. They also strongly believe that the direct communication between the editors and authors are important for the welfare, quality and wellbeing of the Journal and its readers. Therefore, all activities from paper submission to paper publication are controlled through electronic systems that include electronic submission, editorial panel and review system that ensures rapid decision with least delays in the publication processes.

To build its international reputation, we are disseminating the publication information through Google Books, Google Scholar, Directory of Open Access Journals (DOAJ), Open J Gate, ScientificCommons, Docstoc and many more. Our International Editors are working on establishing ISI listing and a good impact factor for IJBB. We would like to remind you that the success of our journal depends directly on the number of quality articles submitted for review. Accordingly, we would like to request your participation by submitting quality manuscripts for review and encouraging your colleagues to submit quality manuscripts for review. One of the great benefits we can provide to our prospective authors is the mentoring nature of our review process. IJBB provides authors with high quality, helpful reviews that are shaped to assist authors in improving their manuscripts.

Editorial Board Members
International Journal of Biometric and Bioinformatics (IJBB)

Dr. Wichian Sittiprapaporn
Mahasarakham University
Thailand

Dr. Paola Lecca
University of Trento
Italy

Associate Professor. Renato Natal Jorge
University of Porto
Portugal

Assistant Professor. Daniela Iacoviello
Sapienza University of Rome
Italy

Professor. Christos E. Constantinou
Stanford University School of Medicine
United States of America

Professor. Fiorella SGALLARI
University of Bologna
Italy

Professor. George Perry
University of Texas at San Antonio
United States of America

Assistant Professor. Giuseppe Placidi
Università dell'Aquila
Italy

Assistant Professor. Sae Hwang
University of Illinois
United States of America

Associate Professor Quan Wen
University of Electronic Science and Technology
China

Dr. Paula Moreira
University of Coimbra
Portugal

Dr. Riadh Hammami
Laval University
Canada

Dr Antonio Marco
University of Manchester
United Kingdom

Dr Peng Jiang
University of Iowa
United States of America

Dr Shunzhou Yu
General Motors Global R&D Center
United States of America

TABLE OF CONTENTS

Volume 6, Issue 1, February 2012

Pages

MR Image Segmentation of Patients' Brain Using Disease Specific a Priori Knowledge

Hassan Tavakkoli   *tavakoli@ibb.ut.ac.ir*
Applied Neuroscience Research Center
Baqiyatallah University of Medical Sciences
Tehran, Iran

Ali Sadeqi   *sadeqi_a@ymail.com*
Applied Neuroscience Research Center
Baqiyatallah University of Medical Sciences
Tehran, Iran

Abstract

Segmentation of high quality brain MR images using *a priori* knowledge about brain structures enables a more accurate and comprehensive interpretation. Benefits of applying *a priori* knowledge about the brain structures may also be employed for image segmentation of specific brain and neural patients. Such procedure may be performed to determine the disease stage or monitor its gradual progression over time. However segmenting brain images of patients using general *a priori* knowledge which corresponds to healthy subjects would result in inaccurate and unreliable interpretation in the regions which are affected by the disease. In this paper, a technique is proposed for extracting *a priori* knowledge about structural distribution of different brain tissues affected by a specific disease to be applied for accurate segmentation of the patients' brain images. For this purpose, extracted *a priori* knowledge is gradually represented as disease specific probability maps throughout an iterative process, and then is utilized in a statistical approach for segmentation of new patients' images. Experiments conducted on a large set of images acquired from patients with a similar neurodegenerative disease implied success of the proposed technique for representing meaningful *a priori* knowledge as disease specific probability maps. Promising results obtained also indicated an accurate segmentation of brain MR images of the new patients using the represented *a priori* knowledge, into three tissue classes of gray matter, white matter, and cerebrospinal fluid. This enables an accurate estimation of tissues' thickness and volumes and can be counted as a substantial forward step for more reliable monitoring and interpretation of progression in specific brain and neural diseases.

Keywords: Brain MR Images, Segmentation, Tissue Classification, Image Registration, A Priori Knowledge, Brain Tissue Probability Maps, Neurodegenerative Disease.

1. INTRODUCTION
Magnetic Resonance Imaging (MRI) [1] of brain is well known as a powerful technique for diagnosis which is widely used by many clinicians to detect structural abnormalities that cause neurological disorders. Until a few years ago, most of the neurologist just employed their personal expertise to inspect a number of cross sections of the patient's brain MRI to diagnosis the disorder or monitor the effects of a specific therapy. Swift progresses in medical image processing [2] have introduced automatic and semi-automatic methods to enable more precise and reliable diagnosis and treatments. Image segmentation [3] is an example for such methods which is widely used in many biomedical applications. A popular application of image segmentation in neurology is partitioning a specific brain structure into three major tissues of gray matter, white matter, and cerebrospinal fluid. Such a segmentation process makes it possible to estimate distributions of different tissue types in the brain in addition to calculate their volumes accurately. This information is very beneficial to make an accurate diagnosis or monitor the treatment progress precisely.

Either manual or automatic Interpretation of brain's high quality images can benefit from utilizing atlases as well as *a priori* knowledge represented as comprehensive probabilistic maps [4, 5]. Brain atlases are three dimensional (3D) images produced by averaging on a large number of brain images of healthy subjects. Probabilistic maps which are frequently represented as 3D images are structures which determine the probabilities by which each voxel of a typical brain image corresponds to any of the major tissue type. Developing advantageous atlases and/or *a priori* knowledge in the forms of inclusive probabilistic maps requires collecting and processing a large set of brain images [6] in addition to utilizing suitable strategies for image registration and warping [7].

Great benefits of employing atlases as well as *a priori* knowledge hidden in probabilistic maps can be extended for analyzing brain images of specific patients with a similar neurological disorder such as neurodegenerative diseases. Neurodegenerative diseases including mild cognitive impairment, Alzheimer [8], and major depression [9, 10], are disorders caused by progressive deterioration of neurons that eventually leads to their death. Clinical symptoms of neurodegenerative diseases include disabilities and dysfunctions resulting in dementia (memory dysfunctions) and/or ataxia (movement disabilities) [11]. Progressive death of neurons in neurodegenerative disease results in atrophy of the brain structures. Such gradual effects can be monitored or even quantified using MRI [12]. The quantification is performed via MR image segmentation and estimating distribution of different brain tissues. Segmentation is usually performed through parametric methods [13] and its precision can be improved using *a priori* knowledge of probabilistic maps registered on the image of patient's brain [14, 15].

Analyzing images of patients' brain using general *a priori* knowledge extracted from brain images of healthy subjects would result in inaccurate and unreliable interpretation in the regions which are affected by the disease [16]. For example in image segmentation of patients' brain, this may result in misclassification of brain tissues and consequently inaccurate measurement of their volumes. As such presentencing a systematic method for development of *a priori* knowledge about structural distribution of brain tissues which is affected by a specific disease and maps is a paramount necessity for more reliable studies on progression of the specific neurologic disorders, and monitoring their gradual affects on different brain tissues.

In this paper a novel technique is proposed for systematically representation of *a priori* knowledge about effects of a specific neurological disease on different tissue structures of the brain. The initial application proposed for the developed knowledge in this paper is segmentation of patients' brain images into its three major tissue types. Such customized segmentation process can also accurately calculate the volumes of each tissue type accurately. Experiments conducted on a large set of images acquired from patients with a similar neurodegenerative disease implied success of the proposed technique for representing meaningful *a priori* knowledge as disease specific probability maps. Promising results obtained also indicated an accurate segmentation of brain MR images of the new patients using the represented *a priori* knowledge, into three tissue classes of gray matter, white matter, and cerebrospinal fluid. This can pave the way for a more precise disease diagnosis, mentoring its gradual growth, and following the treatment progress.

This paper is organized as follows. The required preliminaries are presented in the next section. Section 3 introduces the iterative method used in this paper for development of the disease specific *a priori* knowledge and the segmentation of the brain image of the patients. The experiments conducted and the results obtained are presented in section 4. Finally section 5 discusses the obtained results and concludes this paper.

2. PRELIMINARIES

2.1 Medical Image Registration
In image registration, a one-to-one mapping or transformation is determined between the coordinates of one image space to those in the other. In rigid registration the transformation is

limited to translation and rotation while in affine registration the transformation may also include scaling and shearing. Eq. (1) shows the general form of 3D affine transformation. In this equation T_{Shear}, T_{Scale}, and T_{Rigid} are 4×4 matrices and the a_{ij} parameters are coefficients related to rotation, scaling and shearing, while the t parameters determine translation [17].

$$T_{affine}(x,y,z) = \begin{bmatrix} x' \\ y' \\ z' \\ 1 \end{bmatrix} = T_{shear} . T_{scale} . T_{rigid} . \begin{bmatrix} x \\ y \\ z \\ 1 \end{bmatrix} = \begin{bmatrix} a_{11} & a_{12} & a_{13} & t_x \\ a_{21} & a_{22} & a_{23} & t_y \\ a_{31} & a_{32} & a_{33} & t_z \\ 0 & 0 & 0 & 1 \end{bmatrix} . \begin{bmatrix} x \\ y \\ z \\ 1 \end{bmatrix} \tag{1}$$

While rigid and affine registration are suitable for modeling global motion, they are not capable of modeling local motion which usually occurs in deformable objects such as soft tissue. To model the local motion, non-rigid or deformable registration approaches have been developed.

A Free-Form Deformation (FFD) technique was introduced by Ruckert *et al.* for registering breast MR images [18]. Later, this FFD technique and its modified versions were widely used in other applications of non-rigid image registration by several research groups [19, 20, 21, 22]. FFD models the global and local deformations within the object separately, and then combines them to form an overall smooth deformation. In practice this translates into a global transformation followed by a local transformation:

$$T(x,y,z) = T_{local}(T_{global}(x,y,z)) \tag{2}$$

where T_{global} is a rigid or affine transformation and T_{local} is a deformation model based on B-splines [23].

A modified implementation of the FFD was used in this paper as the non-rigid registration method in the algorithm proposed for generating disease specific probability maps described in Section 3-1. Following the original version of the FFD, let Φ denote an $n_x \times n_y \times n_z$ size mesh of control points ($\phi_{i,j,k}$) with a uniform spacing δ_d in direction d. Also suppose that $\varphi_{i,j,k}$ denotes the displacement of the corresponding control point. Hence, the local transformation can be formulated as a 3D tensor product of 1D cubic B-splines:

$$T_{local}(x,y,z) = (x,y,z) + \sum_{l=0}^{3}\sum_{m=0}^{3}\sum_{n=0}^{3} B_l(u)B_m(v)B_n(w)\,\varphi_{i+l,j+m,k+n} \tag{3}$$

where $\quad i = \left\lfloor \frac{x}{\delta_x} \right\rfloor - 1,\ j = \left\lfloor \frac{y}{\delta_y} \right\rfloor - 1,\ k = \left\lfloor \frac{z}{\delta_z} \right\rfloor - 1,\quad u = \frac{x}{\delta_x} - \left\lfloor \frac{x}{\delta_x} \right\rfloor,\ v = \frac{y}{\delta_y} - \left\lfloor \frac{y}{\delta_y} \right\rfloor,\ w = \frac{z}{\delta_z} - \left\lfloor \frac{z}{\delta_z} \right\rfloor,\quad$ and $B(.)$'s represent the basis functions of B-spline:

$$B_0(u) = \frac{(1-u)^3}{6}$$

$$B_1(u) = \frac{(3u^3 + 6u^2 + 4)}{6}$$

$$B_2(u) = \frac{(-3u^3 + 3u^2 + 3u + 1)}{6} \tag{4}$$

$$B_3(u) = \frac{u^3}{6}$$

As such, the algorithm uses an optimization technique to find the optimum displacements of the control points that yield the best registration in some sense (e.g. maximum similarity).

Considering Eq. 3, the derivative of the deformation field with respect to the B-spline coefficients can be given by:

$$\frac{\partial T_{local}(x,y,z)}{\partial \varphi_{i,j,k}} = B_l(u)B_m(v)B_n(w) \tag{5}$$

where $l = i - \left\lfloor \frac{x}{\delta_x} \right\rfloor + 1$, $m = j - \left\lfloor \frac{y}{\delta_y} \right\rfloor + 1$, $n = k - \left\lfloor \frac{z}{\delta_z} \right\rfloor + 1$ and $B_l(u) = 0$ for *l < 0* and *l > 3*. This implies that the derivative term is nonzero only in the neighbourhood of the corresponding control point. Having such a derivative equation for the transformation, the optimization part of the registration process can be implemented efficiently using an iterative gradient descent or other derivative-based optimization techniques.

2.2   Medical Image Segmentation
Image segmentation is the process of partitioning an image into a number of regions or classes with similar properties based on pre-defined criteria. For example a brain image may be segmented into three soft tissue regions of gray matter, white matter, and cerebrospinal fluid where a more precise qualitative and/or quantitative analysis is made possible. According to [13] segmentation methods are categorized into four major classes:
  1) Thresholding methods
  2) Deformable models
  3) Fuzzy connectivity methods
  4) Statistical techniques
The segmentation technique applied in this paper is a statistical method known as expectation maximization [24, 25]. It is an iterative method through which the maximum likelihood parameters are estimated for segmentation. In summary, the expectation maximization is consists of two iterative steps of calculating the expectation and maximizing it. In the first step, the expectation of the complete data log-likelihood is calculated. In the next step maximum likelihood parameters which maximize the expectation are estimated. These parameters are then applied in the first step of the next iteration. As such, parameters which result in a segmentation with maximum likelihood are progressively obtained via this iterative loop. More details on this method can be found in [24, 25, 26].

3. METHOD
The method proposed in this paper dynamically segment brain MR images of a group of patients with a similar neurological disorder in an iterative process where the disease specific *a priori* knowledge is also extracted concurrently. The extracted *a priori* knowledge corresponds to the distribution of different brain tissues affected by the disease. It would be represented in the form of separate probability maps for gray matter, white matter, and cerebrospinal fluid. The conventional approach for generating brain atlases and probability maps usually perform this task in one single step and by averaging on a number of brain images segmented previously. In the technique proposed in this paper, current simple methods are substituted with an iterative image segmentation process which aims for both enhancing the quality of newly generated probability maps in each iteration a well as improving the precision of input images segmentation simultaneously. The technique applies deformable image registration for adjusting the input images in a reference coordinate, and employs expectation maximization technique for segmenting the patient's brain images. The new probability maps in each iteration are generated by averaging on intensity distribution of images for each specific tissue type. More details on the proposed technique have been provided in the following section.

3.1 Developing Disease Specific *A Priori* Knowledge for Brain Image Segmentation
Expectation Maximization as a parametric approach for image segmentation estimates the intensity distribution for each tissue type in a MR image. Such estimation is performed using *a priori* knowledge represented as probability maps. As such gradual enhancement of probability

maps' quality would progressively results in improving the accuracy of image segmentation as well.

Figure 1 demonstrates schematic structure of the proposed technique for generating disease specific probability maps for each tissue type. As can be seen in this figure the method receives a set of brain MR images of patients with a similar neurological disorder along with a reference brain atlas and its corresponding probability maps as the inputs and consequently goes through the following processing steps:

1) Loading input data including brain MR images of patients as well as reference atlas and probability maps.
2) Initial segmentation for each input image:
    2.1) Registering the reference atlas into the patient's image space.
    2.2) Mapping the probability maps for gray matter, white matter, and cerebrospinal fluid into patient's image space using the transformation function obtained in the previous step.
    2.3) Soft segmentation of the patient's image via expectation maximization method which outputs a patient specific probability map for each tissue type.
3) Entering to the iterative loop for disease specific probability maps generation:
    3.1) Registering each patient's image into the reference atlas space.
    3.2) Mapping each set of patient specific probability maps (obtained in step 2.3 or 3.5) to the reference atlas space using the corresponding transformation function obtained in step 3.1.
    3.3) Averaging patient specific probability maps for each tissue type in the reference space to generate/update the disease specific probability map for the corresponding brain tissue.
    3.4) Transferring new probability maps into each patient's image space using inverse of the transformation function obtained in step 3.1.
    3.5) Soft segmentation of patients' images via expectation maximization method using the new probability maps transformed in step 3.4. The output is a specific set of probability maps for each patient.
    3.5) Return step to 3.2.
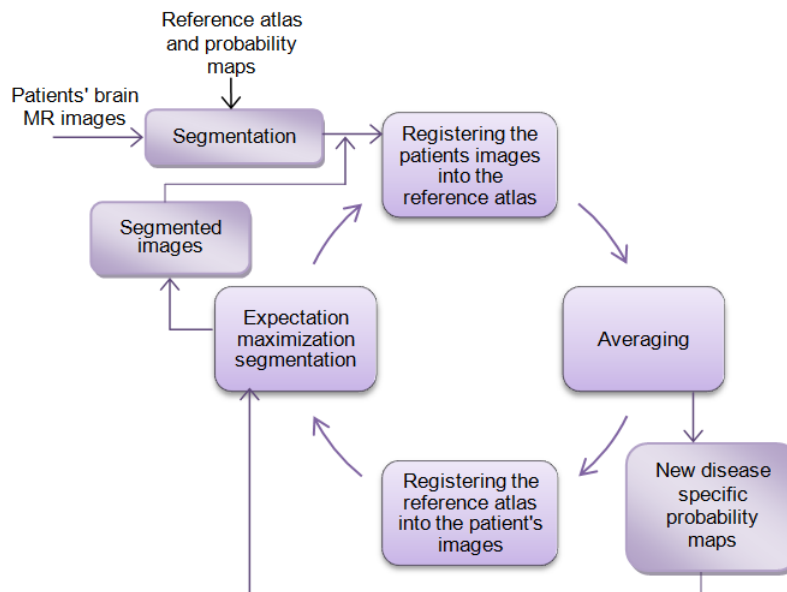

FIGURE 1: Schematic structure of the proposed technique for generating disease specific probability maps as well as segmenting the patients' images.

As mentioned earlier, the processes of generating/updating new disease specific probability maps and improving the precision of patients' image segmentation have been tied together. In other words, for generating/updating disease specific probability maps segmentation of patients' images is a prerequisite, and on the other hand, for a more accurate segmentation of patients' images high quality disease specific probability maps are required. As such, the proposed algorithm employs an iterative loop for generating/updating the disease specific probability maps and in the same loop, applies these new maps for improving the accuracy of segmentation of the patients' brain images. Eventually and after a number of iteration, high quality and precise disease specific probability maps are obtained. Such maps can then be applied for segmenting brain images of new patients accurately where it enables more reliable qualitative and/or quantitative analysis for diagnosis and/or monitoring the disease progress.

4. EXPERIMENTS AND RESULTS

The proposed technique was evaluated on a large set of brain MR images of patients with a similar neurodegenerative disease. The dataset consisted of 108 T1 weighted images of different patients where it was randomly partitioned into two sets of training (98 images) and testing (10 images). The images of training set were used for generating a set of disease specific probability maps for different tissue type, while the never seen images of the testing set were applied for evaluating the performance and accuracy of the generated maps for segmenting brain images of new patients.

Quality of generated probability maps at each iteration of the proposed algorithm was examined by a medical imaging expert. After 6 iterations no major improvement was observed on the quality of generated maps. As such the algorithm's loop was stopped at the end of this iteration and its output was used as the disease specific probability maps for segmentation of new patients' images.

Figure 2 shows the probability maps obtained for the gray matter. The Figure 2(a) demonstrate the initial probability map used as the input of the algorithm in coronal and sagittal planes. Figure 2(b)-(g) present the disease specific probability maps obtained in successive iterations, respectively. As it can be observed, the process of disease specific probability maps generation implies a progressive sharpening of the edges and clarification of the maps. More details may be detected in the probability map images after passing each iteration of the proposed algorithm. Such enhancement may be more appreciated for the images of rows three and four (outputs of second and third iterations). These observations confirm that the generated probability maps enriched with disease specific *a priori* knowledge have rapidly converged toward a similar structure which conforms the disease progress.

In the next stage, the generated disease specific probability maps were applied in the process of image segmentation for new patients' images of the testing set. These never seen brain images had not been presented to the algorithm before. Figure 3 illustrates the typical results obtained for segmentation of gray matter, white matter, and cerebrospinal fluid in one patient's brain image. The figure shows those results obtained by applying the initial probability maps (obtained from healthy subjects' brain images) in the expectation maximization segmentation methods, as well as those obtained through the same segmentation technique by applying the generated disease specific probability maps. Qualitative evaluation performed on the results obtained using the two sets of probability maps suggests that a more precise segmentation has been done using the generated disease specific probability maps. In this case brain tissue structures have been revealed with more meaningful details as well as with less undesirable artifacts via the segmentation process. This can be more appreciated by comparing the two rows of images in Figure 3, and specially in Figure 3(C).

The accuracy of the results obtained for testing set images segmentation using the two sets of initial and generated probability maps was then analyzed quantitatively. For this purpose, the segmentation results obtained using the initial set of probability maps are first corrected manually

in a time consuming process and by a medical imaging expert. The manually corrected segmentation was then used as the reference for evaluating the precision of the segmentation processes performed using the initial and generated probability maps. Two criteria of True Positive Volume Fraction (TPVF) and False Positive Volume Fraction (FPVF) were utilized for the quantitative analysis and evaluations. The average results obtained for gray matter, white matter and cerebrospinal fluid have been reported in Tables 1. The results given in this table imply a considerable increase in the segmentation accuracy of the gray matter, white matter and cerebrospinal fluid by applying the disease specific probability maps generated using the proposed algorithm. In the case of gray matter segmentation, the disease specific *a priori* knowledge could increase TPVF while decreasing the FPVF. Similar results obtained in the case of white matter segmentation as well. In the case of cerebrospinal fluid segmentation, the TPVF has been increase substantially. However it also resulted in a slight increase in FPVF simultaneously. Such increase seems negligible considering the excellent performance of the probability maps in all other cases.
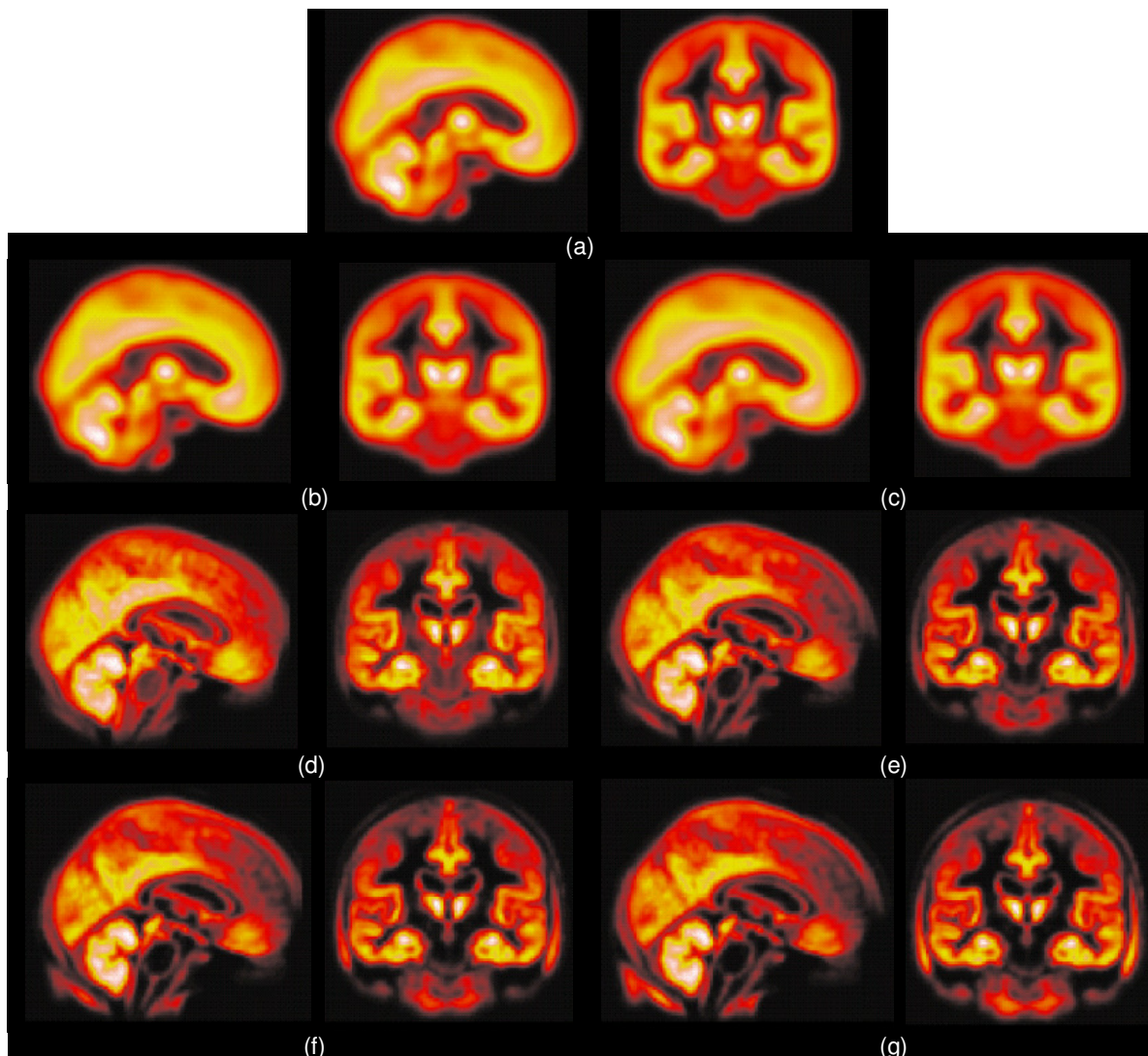

FIGURE 2: Sagittal (left) and Coronal (right) planes of the gray matter probability map. (a): initial probability map, (b)-(g): the neurodegenerative disease specific probability maps, generated in first to sixth iterations of the proposed algorithm, respectively.

5. DISCUSSION AND CONCLUSION

A technique was proposed and evaluated in this paper to extract *a priori* knowledge about structural distribution of different brain tissues affected by a specific neurological disorder from a set of brain MR images of the suffering patients and consequently represented as disease specific probability maps. The disease specific a priori knowledge was then applied in brain image segmentation process of new patients in order to increase the process precision. The processes of generating/updating new disease specific probability maps and improving the precision of patients' image segmentation are mutually contingent on each other. As such, the proposed algorithm utilizes an iterative loop for generating/updating the disease specific probability maps and in the same loop, employs these new maps for improving the accuracy of segmentation of the patients' brain images. Eventually and after a number of iteration, high quality and precise disease specific probability maps are obtained. The obtained maps can then be applied for segmenting brain images of new patients precisely where a more meaningful qualitative/quantitative analysis for diagnosis/monitoring the disease progress is made possible. In addition and utilizing the proposed algorithm, the disease specific probability maps may be made more enriched with further *a priori* knowledge extracted from new sets of patients' images whenever such data is available.
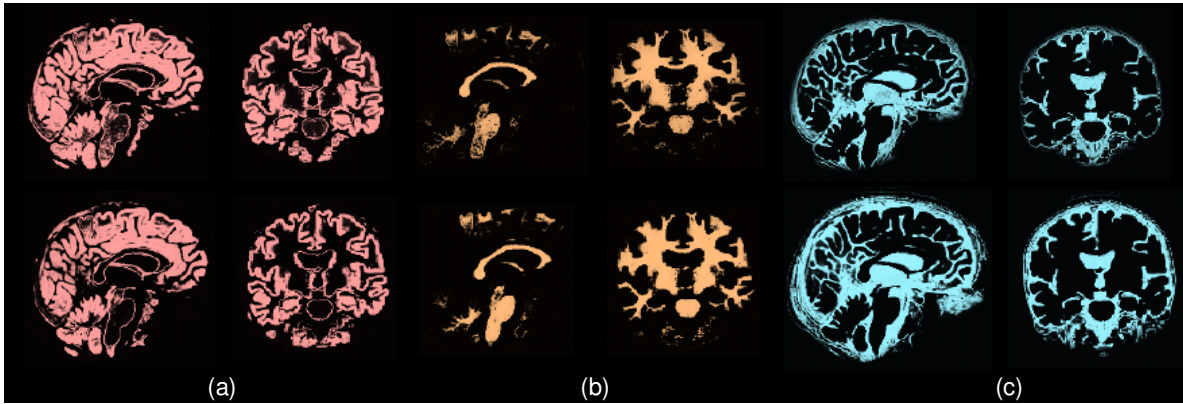
FIGURE 3: Typical results obtained for segmentation of a patient's brain MR image using *a priori* knowledge of the initial probability maps (top row), and the generated disease specific probability maps (bottom row). (a): Gray matter segmentation, (b): White matter segmentation, (c): cerebrospinal fluid segmentation

Brain Tissue	TPVF (Initial probability maps)	TPVF (Disease specific probability maps)	FPVF (Initial probability maps)	FPVF (Disease specific probability maps)
Gray matter	93.9%	97.1%	15.7%	5.4%
White matter	86.8%	92.0%	5.6%	1.9%
Cerebrospinal fluid	70.6%	89.2%	1.9%	2.7%

TABLE 1: Accuracy of different brain tissues segmentation by applying *a priori* knowledge involved in initial (general) and generated (disease specific) probability maps in expectation maximization segmentation algorithm.

The experiments conducted on a large set of MR brain images of patients suffering from a similar neurological disorder confirmed a desirable performance of the proposed method for representing disease specific *a priori* knowledge as well as in employing it for brain image segmentation of new patients. Qualitative evaluation of the generated probability maps implied their high quality conformance with the disease structural progress. The qualitative examinations carried out on the performance of the brain image segmentation of new patients using the generated disease specific probability maps showed a more accurate classification in comparison to the case where a general set of probability maps was used. In the former case, brain tissue structures were

revealed with more meaningful details as well as with less undesirable artifacts throughout the segmentation process. The quantitative evaluations performed on brain image segmentation of new patients also verified a considerable increase in the segmentation precision in the case where the generated disease specific probability maps were applied. Here a favorable increase in TPVF was achieved concurrently with an encouraging decrease in FPVF, in most case.

As mentioned earlier, the immediate goal aimed in this paper for generation and representation of disease specific *a priori* knowledge was brain image segmentation for diagnosing the disease and monitoring/measuring its gradual effects on different brain tissue structures. As such and considering the substantial increase accomplished in the accuracy of the brain image segmentation of new patients using the generated disease specific probability maps, a substantial step has been taken forward towards this goal. This will pave the way for a more reliable disease diagnosis, measuring its progress, and monitoring the treatment response.

6. REFERENCES

[1]   R.W. Brown, M.R. Thompson, E.M. Haacke, R Venkatesan. *Magnetic Resonance Imaging: Physical Principles and equence Design.* New York, NY: John Wiley & Sons Inc, 1999.

[2]   E. Berry. *A Practical Approach to Medical Image Processing.* Leeds, UK: Elizabeth Berry Ltd, 2007.

[3]   D. L. Pham, C. Y. Xu, J. L. Prince.   "Current methods in medical image segmentation". *Annu. Rev. Biomed. Eng.*, vol. 2, pp. 315 - 337, 2000.

[4]   T. M. Peters, D. L. Collins, P. Neelin, A. C. Evans. "Automatic 3D intersubject registration from volumetric data in standardized talairach space". *Journal of Computer Assisted Tomography*, vol. 18, pp. 192-205, 1994.

[5]   A. Evans, P. Fox, J. Mazziotta, A. Toga, J. Lancaster. "A proabilistic atlas of the human brain: Theory and rational for its development". *NeuroImaging*, vol. 2, pp. 89-101, 1995.

[6]   A. W. Toga, J. C. Mazziotta. *Brain Mapping: The Methods.* Burlington, MA: Academic Press, 1996.

[7]   A. W. Toga. *Brain Warping*. Burlington, MA: Academic Press, 1998.

[8]   S.G. Sclan, S. Kanowski. "Alzheimer's disease: Stage-related interventions". *Lippincotts Case Manag*, vol. 6(2), pp. 61-63 , 2001.

[9]   B. L. Roth. "Neuronal Signal Transduction Pathways: Wasteland or the Promised Land?". *Sci. STKE* vol. 45, pp. pe1, 2000.

[10]   H. Anisman, Z. Merali, S. Hayley. "Neurotransmitter, peptide and cytokine processes in relation to depressive disorder: Comorbidity between depression and neurodegenerative disorders". *Prog Neurobiol*, vol. 85, pp. 1-74, 2008.

[11]   C. Brayne, H. Brodaty, L. Fratiglioni, M. Ganguli, k. Hall, K. Hasegawa, H. Hendrie, Y. Huang, C. ferri, M. Prince. "Global prevalence of dementia: a delphi consensus study". *The Lancet*, vol. 366, pp. 2112-2117, 2005.

[12]   C. R. Jack, M. Slomkowski, S. Gracon, T. M. Hoover, J. P. Felmlee, K. Stewart, Y. Xu, M. Shiung, P. C. O'Brien, R. Cha, D. Knopman, R. C. Petersen. "MRI as a biomarker of disease progression in a therapeutic trial of milameline for AD". *Neurology*, vol. 60(2), pp. 253-260, 2003.

[13]   T. Song, E. Angelini, B. Mensh, A. Laine. " Comparison study of clinical 3D MRI brain segmentation evaluation". In Proc. IEEE EMBS '04, 2004, vol. 3, pp. 1671-4.

[14]   J. Talairach, P. Tournoux. *Co-planar stereotactic atlas of the human brain: 3-dimensional proposal system: an approach to cerebral imaging.* Stuttgart, UK: Thieme, 1988.

[15]   A. Toga, P. Thompson. "The role of image registration in brain mapping". *Image and Vision Computing*, vol. 19(1-2), pp. 3-24, 2001.

[16]   D. L. Collins, A. P. Zijdenbos, V. Kollokian, J. G. Sled, N. J. Kabani, C. J. Holmes, A. C. Evans. "Design and construction of a realistic digital brain phantom". *IEEE Trans. on Med. Img.*, vol. 13(3), pp. 463-468, 1998.

[17]   J. V. Hajnal, D. L. G. Hill, D. J. Hawkes. *Medical image registration*, Boca Raton, FL: CRC Press, 2001.

[18]   D. Ruckert, L. I. Sonoda, C. Hayes, *et al.* "Nonrigid registration using free-form deformations: Application to breast MR images". *IEEE Trans. Med. Imaging*, vol. 18(8), pp. 712-721, 1999.

[19]   J. Kybic, M. Unser. "Fast parametric elastic image registration". *IEEE Trans. Med. Imaging*, vol. 12(11), pp. 1427-1441, 2003.

[20]   T. Rohlfing, C. R. Maurer, W. G. O'Dell, *et al.* "Modeling liver motion and deformation during the respiratory cycle using intensity-based nonrigid registration of gated MR images". *Med. Phys.*, vol. 31(3), pp.427-432, 2004.

[21]   J. R. McClelland, A. G. Chandler, J. M. Blackall, *et al.* "4D motion models over the respiratory cycle for use in lung cancer radiotherapy planning", In Proc. SPIE 5744, 2005, pp. 173–183.

[22]   J. R. McClelland, J. M. Blackall, S. Tarte. "A continuous 4D motion model from multiple respiratory cycles for use in lung radiotherapy". *Med. Phys.*, vol. 33(9), pp. 3348-58, 2006.

[23]   S. Lee, G. Wolberg, S. Y. Shin. "Scattered data interpolation with multilevel B-splines*". IEEE Trans. Visualization Comput. Graph.*, vol. 3, pp. 228–244, 1997.

[24]   K. Van Leemput, F. Maes, D. Vandermeulen, P. Suetens. "Automated model-based bias field correction of MR images of the brain". *IEEE Trans. Med. Img.*, vol. 18(10), pp. 885-896, 1999.

[25]   K. Van Leemput, F. Maes, D. Vandermeulen, P. Suetens. "Automated model-based tissue classification of MR images of the brain". *IEEE Trans. Med. Imag.*, vol. 18(10), pp. 897-908 , 1999.

[26]   B. Flury. *A first course in multivariate statistics.* New York, NY: Springer- Verlag, 1997.

Mr. Hamid M. Hasan , Prof. Dr. Waleed A. AL.Jouhar & Dr. Majid A. Alwan

3-D Face Recognition Using Improved 3D Mixed Transform

Mr. Hamid M. Hasan   *Hamid2012net@gmail.com*
College of Eng./ Electrical Eng. Dept.
Basra University
Basra , Iraq

Prof. Dr. Waleed A. AL.Jouhar   *Profwaleed54@yahoo.com*
College of Eng. /Electrical Eng. Dept.
Baghdad University.
Baghdad , Iraq

Dr. Majid A. Alwan   *Altimimee@yahoo.com*
Electrical Eng. Dept
Basra University, college of Eng.
Basra , Iraq

Abstract

This paper deals with the using of Improved 3D Mixed Transform (3D-IMT) for face recognition problem. The mixed transform consists Fourier based 3D radon transform plus 1-D Wavelet transform (which is also known as 3D Ridgelet transform). The Mixed Transform is improved by using the Particle swarm optimization (PSO) technique. The improvement involves the selection of the best of directions for smart rectangle-to-polar transform as a part of the 3D Radon Transformation. The 3D-IMT is applied to the 3D representation of face images, and yields a few number of features, these features is projected into the maximized projection that achieves good recognition rate using the Linear Discriminant Analysis (LDA).

Keywords: Face Recognition, 3-D Radon Transform, Particle Swarm Optimization (PSO), Wavelet Transform ,Linear Discriminate Analysis (LDA) .

1. INTRODUCTION

1.1. Face Recognition Problem

Face recognition is one of the most important biometrics which seems to be a good compromise between actuality and social reception and balances security and privacy well. It has a variety of potential applications in information security law enforcement, access controls. Face recognition systems fall into two categories: verification and identification, Face verification is 1:1 match that compares a face images against a template face image. On the other hand face identification is 1:N problem that compares a probe face image against all image templates in a face database. Face recognition is a very difficult problem due to a substantial variation in light direction (illumination) , different face poses , and diversified facial expressions, Aging (changing the face over time), Occlusions (like glasses, hair, cosmetics) , so building an automated system that accomplishes such objectives is very challenging. In last decade many systems with recognition rate greater than 90% has been done. However a perfect system with 100% recognition rate remains a challenge. Face recognition algorithms are divided by [1,2] into three categories, as follows:-

1. Holistic methods: These methods identify a face using the whole face images as input and extract the overall features.
2. Feature based methods: these methods used the local facial features for recognition (like eyes , mouths, fiducial points ..etc.)

3. Hybrid methods: these methods used both feature based and holistic features to recognize a face. These methods have the potential to offer better performance than individuals.

1.2. Three Dimensional (3D) Face Recognition

The vast majority of Researches deal with methods based on 2D image processing using intensity or color images which reached higher than 90% recognition rate under controlled lighting conditions whoever the performances drop in case of pose, illumination and expression variation. Almost the 2D techniques still encounters many difficulties. On the other hand the three dimensional (3D) face recognition technologies is now emerging, in part, due to the availability of improved 3D imaging devices and processing algorithms. The main argument in favor of using 3D information for face recognition appears to be that it allows us to exploit feature based on shape and the curvature of the face without being plagued by the variances caused by lighting also the pose variation can be corrected by rigid rotations in 3D space they also provide structural information about the face (e.g., surface curvature and geodesic distances) which cannot be obtained from a single 2D image. The 3D face recognition algorithms can be broadly classified into three groups [3], first, there are the 3D appearance based techniques these techniques include the statistical methods like PCA and 3D PCA, ICA, LDA, 3D techniques based on ICA and LDA have been reported to perform better than 3D PCA. The second class use a 3D facial surfaces to represents individuals these 3D models are rotated and translated using Iterative Closest Point (ICP) algorithm the ICP based algorithms are reported to be robust to variable facial poses and illumination the expression variation can be deal with using intrinsic representation of facial surfaces. The third class is the local feature based 3D face recognition techniques that employ structural properties of local regions of the 3D face. Some of techniques in this class employ facial profiles for matching 3D faces it is reported that the central vertical facial profile has been noted to be effective at uniquely identifying individuals. Other using local geometric characteristics of facial sub regions including their positional coordinates, surface areas and curvatures , and the 3D Euclidean distances, ratios of distances, joint differential invariants, and angles between the local facial regions. A few attempts have been made to automatically locate facial landmarks on 3D models using surface. A number of techniques based on local facial features have been reported to perform better than 3D PCA and ICP [4].

1.3. Three Dimensional (3D) Image Representation Techniques

Two main representations are commonly used to model faces in 3D space [5]. These are the Point clouds or triangulated surface meshes and Range Images (also referred to as a 2.5D surface or depth map). The point cloud representation contains the (x, y, z) coordinates of a set of points on the facial surface. A range image consists of (x, y) points on a regular rectangular grid each (x, y) point is associated with a z value of the point on the surface closest to the acquisition device. The Techniques which are currently being used to obtain 3D information include [6]:-

• Scanning systems: using Laser face scanner.
• Structured light systems: These systems make use of the principles of stereo vision to obtain the range data.
• Stereo vision systems: These systems that attempt to extract 3D information from two or more 2D images taken from different angles.
• Reverse rendering/shape from shading.

1.4. A Brief Historical Review of 3D Faces Recognition

Many surveys has been published [6,7,8] about the 3D Face Recognition most papers report performance as rank-one recognition rate although some report equal-error rate or verification rate at a specified false accept rate but on a limited number of persons and only a few have dealt with data sets that explicitly incorporate pose and/or expression variation.

Cartox et al. [9]approached 3D face recognition by segmenting a range image based on principal curvature they reported 100% recognition rate for either in small data set (5 persons and database size was 18 images).

Nagamine et al.[10] approach 3D face recognition by finding five feature points, using those points to standardize face pose.

Experiments are performed for 16 subjects with 10 images per subject the reported performance was 100% but the computational requirements were apparently regarded as severe.
Hesher et al. [11] explore PCA style approaches the image data set has six different facial expressions for each 37 subjects the reported performance is 97%.
Lu et al.[12] , using ICP-based approach performed on point set Images the approach assumes that the gallery 3D image is a more complete face model and the probe image is a frontal view that likely a subset of gallery image. In experiment with 18 persons a recognition rate of 96% was reported.

Russ et al.[13] presented results of Hausdorff matching on range images they used portions of FRGC v1 dataset they reported 98% as a probability of correct verification.

Chang et al. [14] describe a "multi-region" approach to 3D face recognition. It is a type of classifier ensemble approach in which multiple overlapping sub regions around the nose are independently matched using ICP and the results of the 3D matched are fused. The experimental evaluation using the FRGC v2 data set was conducted in which one neutral-expression image is enrolled as the gallery for each person. Performance of 92% rank-one recognition rate was reported.
Passalis et al.[15] described an approach to 3D face recognition that uses annotated deformable models. An average 3D face is computed on a statistical basis from a training set. Landmarks are selected based on descriptions by Frakas. Experimental results are presented using the FRGC v2 data set. For an identification experiment in which one image per person is enrolled in the gallery (466 total) and all later images(3541) are used as a probe, performance reaches nearly 90% rank-one recognition.

Gupta S. et al.[3] they present a novel anthropometric 3D (Anthroface 3D) face recognition algorithm. It is a completely automatic face recognition algorithm that employs facial 3d Euclidean and geodesic distances between 10 automatically located anthropometric facial fiducial points and a linear discriminant classifier. On a database of 1149 facial images of 118 subjects the EER=1.98% and rank one recognition rate of 96.8% was achieved.

Sina Jahanbin et al.[16] They present a novel identity verification system based on Gabor features extracted from range image . Multiple landmarks (fiducials) on face are automatically detected the Gabor features on all fiducials are concatenated to form a feature vector then the LDA is used. The novel features were tested on 1196 range images from Texas 3DFRC database the reported EER was 2.2%.

Hengliang Tang et al.[17] They presented a novel 3D face recognition algorithm based on sparse representation. First, a 3D face normalization deal with the raw faces. Then, three types of facial geometrical features are extracted to describe the 3D faces after that a feature ranking is performed using (FLDA). Finally, the sparse representation framework is used to collect all the face features. The experiments tested on the BJUT-3D and FRGC v2 databases. The reported recognition rate is 95.3% for the method of fusing the three types of features.

2. THE PROPOSED METHOD
Our approach for 3D Face Recognition is depicted in figure (1). The range Images were used from the Texas3DFR Database [38]. Firstly, the images were preprocessed by interpolation method in order to remove the holes due to spikes these Range images are translated into 3D space using topography representation as 3D array these 3D data is transformed into 3D Radon space using 3D Radon Transform (3DRT). The (3DRT) is optimized by Particle Swarm Optimization (PSO) to select the best directions (i.e. θ, $\square$). These directions achieve a high recognition rate as well as the minimum number of features. The selected features in Radon

space is translated into two parts using 1-D Wavelet Transform then only one part is selected so only a half number of features are used. These features are projected into maximized discriminate projection using Linear Discriminant Analysis (LDA).
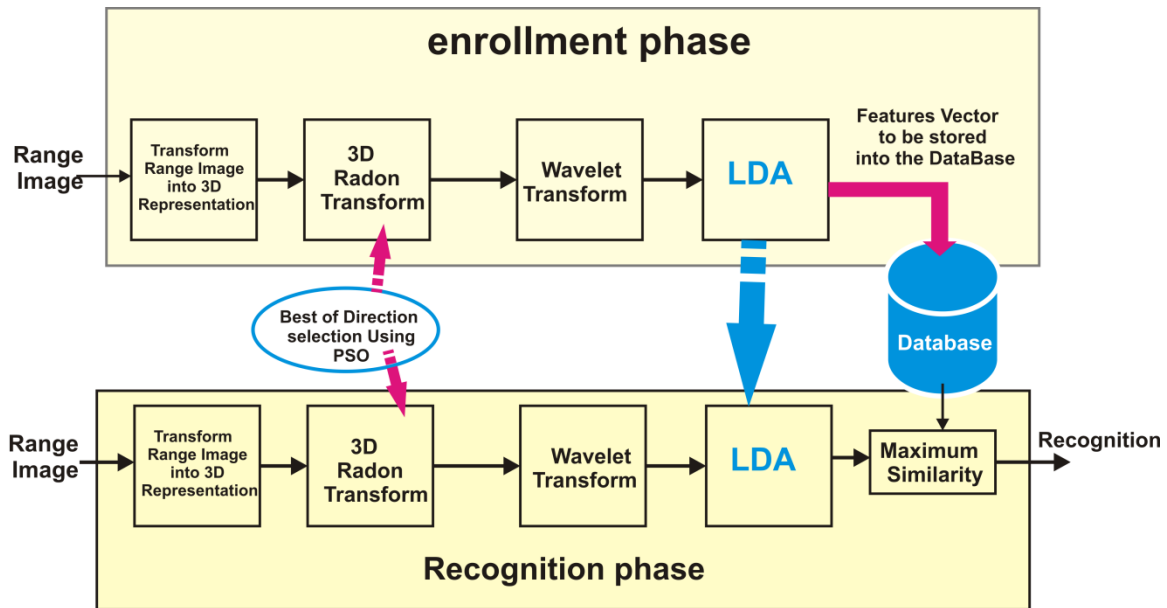

FIGURE 1: The system block diagram.

2.1 The 3D Radon Transform

2.1.1 Introduction
The 3D Radon Transform integrates on planes. Let f(X) be a three dimensional signal where X=[x, y, z]. Let, also ζ be a unit vector in R3 and ρ a real number. The 3D Radon Transform RT(ζ , ρ) of the f(x), is a function which associates to each pair (ζ , ρ) the integral of f(x) on the plane Π(ζ , ρ)={x | x . ζ=ρ } [18] .
The 3D Radon Transform is given by the formula:

$$RT(\zeta , \rho) = \int_{-\infty}^{+\infty} f(x)\delta(X.\xi - \rho)dx \qquad (1)$$

Since ζ can be written in spherical coordinates as ζ=[cos□sinθ ,sin□cosθ,cosθ] then equation (1) can be rewritten:

$$RT(\rho,\theta,\square) = \int_{-\infty}^{+\infty}\int_{-\infty}^{+\infty}\int_{-\infty}^{+\infty} f(x,y,z) . \delta(x\cos\emptyset\sin\theta + y\sin\emptyset\sin\theta + z\cos\theta - \rho)dxdydz \qquad (2)$$

Each value of the RT(ρ,θ,□) expresses the summation of the values of f(x,y,z) which lie on the plane defined by the parameters (ρ,θ,□).

2.1.2 Radon Transform Using Fast Fourier Transform
A tight relationship exists between Fourier transform (FT) and Radon transform (RT) of a function. The 1D FT of n-dimensional RT(f) along the radial direction ρ represents a radial sampling of the n-dimensional FT of f. This is the central-slice theorem. With the central-slice theorem the 3D Radon transform can be computed equivalently by performing a 3D DFT, a Cartesian-to-polar mapping, and a 1D DFT. This process requires 3D interpolation in real space which is a computation intensive. The computing cost is substantially reduced in a two-step process. In the

first step rotate the structure stepwise around one axis and obtain a set of projections. In the second step compute the 2D Radon transform of each projection.

2.1.3 Particle Swarm Optimization (PSO)

PSO was firstly introduced by Kenny and Eberhart in 1995 [20] it is one of the evolutionary computation technology based on swarm intelligence. In a PSO system each solution called a "particle". Particles fly around in the problem search space to look for the optimal solution. Each particle adjusts its position according to the flying experience of its own and the experience of neighboring particles. Each particle updates its velocity and position using the following equation [21]:-

$$V_i(k+1) = V_i(k)+c1 * rand1(pbest(k) - X_i(k)) + c2* rand2(gbest(k) - X_i(k)) \qquad (3)$$

$$X_i (k+1)=X_i(k) + V_i(k+1) \qquad (4)$$

Where ,

V_i	is called the velocity for particle i;
X_i	is represent the position of particle i ;
Pbest	is the best position of ith particle ;
gbest	is the global best position ;
rand	is random variable in [0,1];
c1 and c2	are the learning factors;
w	is called the inertia weight .

To search for optimal solution each particle changes its velocity according to Eq (3). The value of V_i is clamped to the range [Vmin, Vmax] to avoid excessive roaming of particle outside the searching space. Then each particle moves to a new potential solution using Eq. (4). This process is repeated until a stopping criterion is reached. The above equations (3,4) are the basic Equation and not guarantee the global solution is reached and may trapped in local minima. To avoid the local minima there are many variations for the basic equations have been suggested like (QPSO) which adding quantum behavior to basic PSO[22,23,24], (CPSO) which add chaotic[25] through chaos maps to basic PSO also the mixing of the two previous methods is suggested in [23] , There are an efforts to add the crossover and mutation used in GA to be used with PSO which improve its behavior and avoids the local minima[26]. Also a varying dimensional particle swarm optimization (VD-PSO) was proposed by Yanjun Yan[27]. An improved PSO by estimation of distribution was introduced in[28].

Some of PSO applications in the Face Recognition field are feature selection optimization[29], Robust object detection scheme using Binary PSO[30], A Novel Evolutionary Face Recognition using PSO[31], Face Recognition Using shift invariant feature transform and BPSO[32], Face Recognition by Extending EBG matching using PSO[33], using CPSO-SVM in Face Recognition [34], Holistic and partial facial fusion by BPSO[35].

In our project the PSO is used to select the best values of (θ, □) for 3D Radon transform; that achieve the high recognition rate. The range of (θ, □) for 3D Radon transform is (-π to π) but due to symmetry of the transform we can calculate only in range (-π/2 to π/2). Also for discrete RT only the integer values are used. We used the PSO to select the minimum number of angles (θ, □) required to obtain the best recognition rate. A novel method of encoding the parameters (θ, □) within the particle was used which led to a reduced number of computations that are required by 3D Radon.

2.1.4 Wavelet Transform

The continuous wavelet transform (CWT) is defined as the sum over all time of the signal multiplied by scaled, shifted versions of the wavelet function ψ:

$$C(\text{scal}, \text{position}) = \int_{-\infty}^{+\infty} f(t)\psi(\text{scal}, \text{position}) \qquad (5)$$

The results of the CWT are many *wavelet coefficients* C which are a function of scale and position calculating wavelet coefficients at every possible scale is a fair amount of work, and it generates an awful lot of data. What if we choose only a subset of scales and positions that if we choose scales and positions based on powers of two so called *dyadic* scales and positions then our analysis will be much more efficient and just as accurate[36]. An efficient way to implement this scheme using filters was developed in 1988 by Mallat. The Mallat algorithm is in fact a classical scheme known in the signal processing community as a *two-channel sub band coder* for many signals and the low-frequency contents is the most important part. It is what gives the signal its identity. On the other hand the high-frequency contents impart flavor or nuance In wavelet analysis. We often speak of *approximations* and *details*. The approximations are the high-scale low-frequency components of the signal. The details are the low-scale high-frequency components see figure (2). In our project only the approximations signal (A) is used and the details signal (D) is ignored this achieves two goals. The first is that the features produced will maintain a high classification rate. The second is the number of features are reduced into one half. The mother wavelet (ψ) used is Daubechies (db1) also known as Harr which has been proven effective for image analysis and feature extraction.

Basic Level DWT
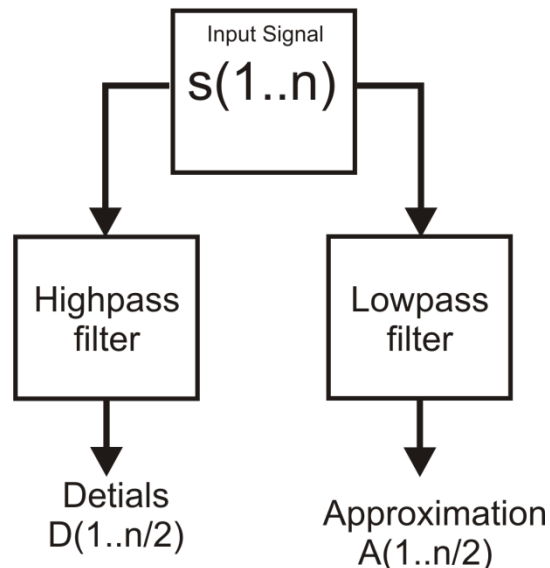
FIGURE 2: Level one Discrete Wavelet Transform (DWT)

2.1.5   Linear Discriminant Analysis (LDA)

The LDA finds a set of basis vectors which maximizes the ratio of the between-class scatter and within–class scatter [37]. Given N samples of C classes and let N_i be the number of samples in the *ith* class(ci). let Mt be the mean of the whole data set and mi be the mean of the *ith* class (ci) then the between-class scatter matrix is defined by:

$$S_B = \sum_{i=1}^{c} N_i(mi - Mt) \ (mi - Mt)^T \qquad (6)$$

And the within-class scatter matrix is defined by

(7)

Then the basis vectors is:

$$\overline{\qquad}$$ (8)

3. THE EXPERIMENTS

Three different experiments were conducted using Texas 3DFR Database [38]. The Texas 3D Face Recognition Database contains 1149 range and portrait mage pairs of adult human subjects each image is (751 x 501) 8-bit. A Sample image and its 3D representation is shown in figure (3).The database images are scaled down into (94 x 63). Each scaled image is transformed into 3D space as (94, 63, 90) array of real numbers these 3D arrays were transformed into 3D radon space as (90, 90, 90) real numbers. This means that each image is represented as (729000) real numbers. A features vector of length (90) real numbers was selected from (72900) real numbers by using PSO. Those (90) value vectors was further reduced into (45) value vectors after Wavelet Transform. These feature vectors were projected into the maximized discrimination projection using the Linear Discriminante Analysis (LDA) and stored into the database .
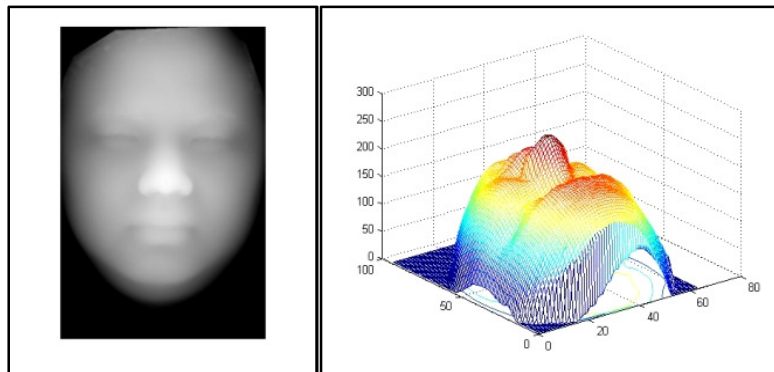
FIGURE 3: left one is the Range Image and right one is the 3D representation of the left.

3.1. Experiment No.1

In this experiment 100 subjects were selected with two different images for each subject one for the gallery and one as a probe image for testing. In this experiment the LDA stage is not used because there is only one sample per class is used. The other stages depicted in fig(1) were used. The recognition rate achieved conducting this experiment was RR=86% .

3.2. Experiment No.2

In this experiment 18 subjects were selected with 10 images per subject as a gallery and more than 10 images as a probe. The gallery set and probe set are disjoint; see figures (4, 5). The complete system was used In this experiment. The recognition rate achieved was 100%.
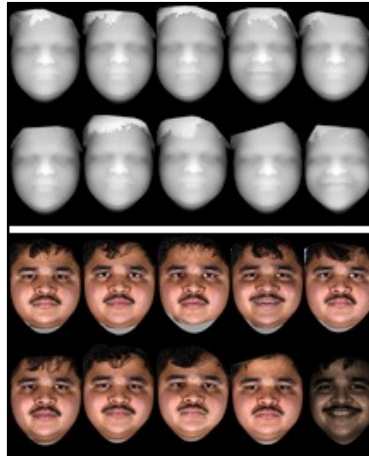
FIGURE 4: The upper 10 range images are a samples of images for a person used in the gallery , the lower 10 are the portrait for the same range images in the upper part.
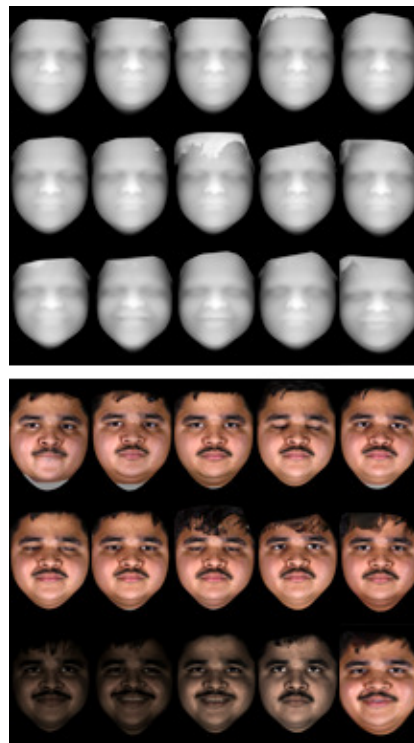
FIGURE 5: The upper range images are a samples of images for a person used as Probes , the lower are the portraits for the same range images in the upper part.

3.3. Experiment No.3

In this experiment an (18) subjects were used with 10 images per subject as a gallery. The probe set was composed of 180 images for authorized users   and 180 image for imposters (not authorized). All sets were disjoint . The Receiver Operating Condition ROC was illustrated by the figure(6). The verification rate is 98.34% or (FRR=1.66% , at zero FAR).

Mr. Hamid M. Hasan , Prof. Dr. Waleed A. AL.Jouhar & Dr. Majid A. Alwan
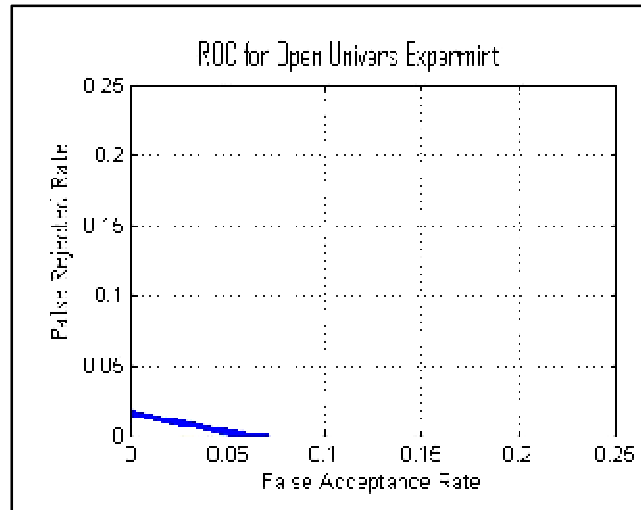
FIGURE 6: Receiver Operating Condition for experiment 3

4. DISCUSSION AND COMPARATIVES

The first and second experiments are recognition test for our method and the third one is for verification test. The results are promise and even the comparison in not easy task because the many differences between evaluation scenarios due to the different data set available and different scenarios in partitioning those data sets between training and gallery and probe data sets but we can depict the validity of our work as following

A. The first and second experiments can be compared with some related works as shown in table(1). Some works used a controlled environment for the data set (i.e. equal in illumination and pose and expression) some other not. The images we used are selected randomly from the data base with different conditions.

B. The third experiment can be compared with some related works as shown in table(2). Some of them follow the Face Recognition Grand Challenge (FRGC V2.0) ROC III protocol they report the False Rejection Rate (FRR) at False Acceptance Rate (FAR) equal to 0.1%. We report the Equal Error Rate (EER=1.3%) and the FRR=1.64% at FAR=0.1% and FRR=1.66% at FAR=0%.

 All the experiments are carried out using MATLAB software R2010a on a laptop computer with i3 CORE @ 2.4 GHz speed and 2 GB RAM. The time required to process one image approximately equal to 5.56 msec and to process all the 180 images to be stored in the gallery was approximate to 1 sec. The recognition or verification time is a faction of second and depends on the size of the data base used which must be investigated further. Also this method need to be tested on large data set that agrees with the used scenario to test its validity.

author	database	#subject	#Training images	#Gallery images	#Probe images	Performance
Chang[41]	Notre Dame	166	278	1/subject controlled	1/subject controlled	RR= 83.7%
Godil [42]	CAESAR	200	-	1/subject	1/subject	RR= 68%
Gupta[40]	Texas 3DFR	12	360	1/subject neutral	29/subject	RR= 98.6%
Gupta[39]	Texas 3DFR	105	-	1/subject neutral	663	RR=98.64%
Our experiment(1)	Texas 3DFR	100	No training	1/subject uncontrolled	1/subject uncontrolled	RR = 86%
Our experiment(2)	Texas 3DFR	18	180	10/subject uncontrolled	10+/subject uncontrolled	RR=100%

TABLE 1: A Comparison between some reported Face Recognition rates and the recognition rate in experiment 1&2.

Author	#subjects	#Gallery images	#Probe images	Performance
Passalis [15]	466 FRGC v0.2	4007	4007	FRR = 3.6% FAR = 0.1%
Husken [43]	466 FRGC v0.2	4007	4007	FRR = 2.7% FAR = 0.1%
Maurer [44]	466 FRGC v0.2	4007	4007	FRR = 6.5% FAR = 0.1%
Jahanbin[16]	109	109	382 + 424 imposters	EER= 2.2%
Our experiment(3)	18	180	180 + 180 imposters	FRR=1.64% FAR=0.1% EER=1.3%

TABLE 2: Comprison between some reported Face Verification rates and the Verification rate in experiment 3.

5. CONCLUSIONS

In this work an Improved 3D Mixed Transform (3D IMT) is used for 3D face recognition. The 3D mixed Transform is also known as 3D Ridgelet Transform. It is composed of 3D Radon Transform (3DRT) plus 1D Wavelet Transform. The 3D Radon that we are used is Fourier based. This transform is improved by using (PSO) to select the best directions (θ, □) along which the 3DRT is performed. By this method the number of features is reduced to a vector of (45) elements as well as achieved a maximized discrimination based on the Linear Discriminant Analysis (LDA) as a consequence this leads to a high recognition rate. Three experiments were conducted:

1. In the first experiment a single image per person (i.e. a vector of 45 elements) is stored in the database and another one is used for testing. The gallery set and probe set were disjoined. The number of subjects used were 100 and the recognition rate was RR=86%.
2. In the second experiment ten images per person are used for training and more than ten for testing. All images have different expressions, illuminations and poses. The training and testing sets are non-overlapped. The number of subjects used were 18 subjects and the recognition rate was RR=100%.
3. The third experiment was the same of the experiment 2 but the test set was different. Her test set contains 180 imposters (no subject is stored in the database) and 180 images of authorized subjects (stored in the database). The Receiver Operating Condition (ROC) is illustrated in figure (6). The verification rate is 98.34% or (False Rejection Rate (FRR) =1.66 % at zero False Acceptance Rate).

Mr. Hamid M. Hasan , Prof. Dr. Waleed A. AL.Jouhar & Dr. Majid A. Alwan

6. ACKNOWLEDGMENT

7. REFERENCES

[1] Nilima B. Kachare, Vandana S. Inamdar, 2010, " Survey of Face Recognition Tecchniques", International Journal of Computer Applications(0975-8887), Volum 1-No.19,2010.

[2] Patil A.M., Kolhe S.R. and Patil P.M., 2010,"2D Face Recognition Techniques:A Survay", International Journal of Machine Intelligence.

[3] Gupta,S. Mia K. Markey and Alan C. Bovik,2010, " Anthropometric 3D Face Recognition", Int. J. Comput. Vis, Springer Science+Business Media LLC 2010.

[4] Irfanoglu, M. O. Golberk, B., & akarun L.(2004)." 3D shape based face recognition using automatically registered facial surfaces", in proceeding of the 17th international conference on pattern recognition, IEEE computer Society.

[5] Andera F. Abate, Michele Nappi, Daniel Riccio, Gabriele Sabatino, 2007, "2D and 3D face recognition: A survey", Pattern Recognition Letters 28(2007) 1885-1906.

[6] Rabia Jafri and Hamid R. Arabnia , 2009,"A Survey of Face Recognition Techniques", Journal of Information Processing systems, Vol 5, No.2, June 2009.

[7] Kevin W. Bowyer, Kyong chang, Patrick Flynn, 2006, " A survey of approaches and challenges in 3d and multi-modal 3D+2D face recognition", Computer Vision and Image Understanding 101(2006) 1-15.

[8] Gupta,S. Mia K. Markey and Alan C. Bovik,2007 ," Advances and Challenges in 3D and 2D+3D Human Face Recognition", In Pattern Recognition Research horizons, New York: Nova Science.

[9] J. Y.Cartoux, et al., 1989," Face authentication or recognition by profile extraction from range images, in: proceedings of the Workshop on interpretation of 3D Scenes, 1989, pp.194-199.

[10] T. Nagamine, et al. "3D facial image analysis for human identification, in International Conference on Pattern Recognition (ICPR 1992), pp.324-327.

[11] C. Hesher, et al." A novel Technique for face recognition using range imaging", in: Seventh International Symposium on Signal Processing and Its Applications",2003 , pp.201-204.

[12] Lu et al.,"Matching 2.5D scans for face recognition " in: International conference on Patteren Recognition(ICPR 2004),pp.362-366.

[13] Russ et al."3D facial recognition: a quantitative analysis, in 45-th Annual Meeting of the Institute of Nuckear Material Management (INMM), July 2004.

[14] Chang et al."Adaptive rigid multi-region selection for handling expression variation in 3D face recognition, in IEEE Workshop on Face Recognition Grand Challenge Expermints, June 2005.

[15]   Passalis, et al." Evaluation of face recognition in presence of facial expressions: an annoted deformable model approach, in: IEEE Workshop on FRGC Expermints, June,2005.

[16]   Jahanbin S. et al."Automated facial Feature Detection and Face Recognition using Gabor Features on Range and Portrait Images",2008,(ICIP 2008),pp.2768-2771.

[17]   Tang H. et al. 2011" 3d face recognition based on sparse representation", J. Supercomputer 58:84-95. Springer science+Business Media. LLC 2010.

[18]   Dimitrio Zarpalas, et al., 2004," 3D Model Search and Retrieval Based on the 3D Radon Transform",IEEE Communication Society.

[19]   Slvatore lanzavicchia and pier luigi " fast computation of 3D Radon Transform via a direct Fourier method",BIOINFORMATICS, vol.14 no.2 ,1998 pp212-216.

[20]   Alec Banks, et al. " A review of particle swarm optimization. Part II: hybridization, combinatorial, multicriteria and constrained optimization, and indicative applications", Nat Comput (2008) 7:109-124, DOI 10.1007/s11047-007-9050-z.

[21]   Shih wei Lin and shih chieh Chen, " PSOLDA: A particle swarm optimization approach for enhancing classification accuracy rate of linear discriminant analysis", Applied Soft Computing 9 (2009) 1008-1015.

[22]   Millie Pant et al, "A New Quantum Behaved Particle Swarm Optimization",GECCO'08,July 12-16, 2008 Atlanta, Georgia. USA.

[23]   Leandro dos Santos Coelho," A quantum particle swarm optimizer with chaotic mutation operator", Chaos, Solutions and Fractals 37 (2008) 1409-1418.

[24]   O. Togla altinoz, et al. " Chaos Particle Swarm Optimization PID Controller for the Inverted Pendulum System", 2nd International Conference on Engineering Optimization, September 6-9, 2010, Lsbon, Portugal.

[25]   Leandro dos Santos Coelho and Viviana Cocco Mariani, " A novel chaotic particle swarm ooptimization approach using Henon map and implicit filitering local search for load dispatch", Chaos, Solutions and Fractals 39(2009) 510-518.

[26]   Qing Zhang, et al. " Fast Multi swarm Optimization with Cauchy Mutation and Crossover operation", Puplications of China University of Geosciences, School of Computer, Wuhan, P.R.China, 430074.

[27]   Yanjun Yan and Lisa ann Osadciw, "Varying Dimensional Particle Swarm Optimization", 2008 IEEE swarm Intelligence symposim , St. Louis Mo USA, September 21-23,2008.

[28]   R. V. Kulkarni and G.K. Venayagamoorthy, " An Estimation of Distribution Improved Particle Swarm Optimization Algorithm", ISSNIP 2007.

[29]   Yanj Yan, Ganapathi Kamath and Lisa ann Osadciw, " Feature Selection Optimization by Discrete Particle swarm Optimization for Face recognition", Syracuse University , Syracuse , NY, USA 13244.

[30]   Hong Pan, LiangZhengXia, and Truong Q.Nguyen," Robust Object detection Scheme using feature selectin", Proceeding of 2010 IEEE 17th International Conference on Image Processing , September 26-29, 2010, Hong Kong.

Mr. Hamid M. Hasan , Prof. Dr. Waleed A. AL.Jouhar & Dr. Majid A. Alwan

[31] Osslan Osiris Aergara Villegas and Viancy Guadalupe," a Novel Evolutionary Face algorithm Using Particle Swarm Optimization ", 2009 Fith International Conference on Signal Image Technology and Internet Based Syetems.

[32] Lanzarini Laura , et al. " Face Recognition Using SIFT and Binary PSO Descriptors", 2010 Proceedings of the ITI 2010 32th Int. Conf. on Information technology Interfaces, June 21-24,2010, Cavtat, Croatia.

[33] Rajinda Senaratne, et al. " Face Recognition by Extending Elastic Bunch Graph Matching with Particle Swarm Optimization", Journal of Multimedia , VOL. 4, No. 4, August 2009.

[34] Ming Li, et al. " Application of Improved CPSO-SVM Approach in Face Recognition", 2009 Internaltional Conference on Artificial Intelligence and Com[utational Intelligence.

[35] Xiaorong Pu, Zhang YI, Zhongjie Fang," Holistic and partial facial features fution by binary particle swarm optimization", Neural Comput & Applic (2008) 17:481-488.

[36] C.Valens,1999-2004,"A Really Friendly Guide to Wavelets", ,available on Internet, questions goto wavelets@polyvalens.com.

[37] Belhumeur PN, Hespanala JP, Kriegman DJ (1997) Eigenfaces vs. fisherfaces: recognition using class specific linear projection. IEEE Trans Pattern Anal Mach Intell 19(7):711-720.

[38] Gupta, S. et al., 2010,"Texas 3D face recognition database", In Image analysis and interpretation ,2010 IEEE southwet symposium on, Austin,TX.

[39] S. Gupta, M. K. Markey, J. K. Aggarwal, and A. C. Bovik. Three dimensional face recognition based on geodesic and euclidean distances. In Electronic Imaging, Vision Geometry XV, volume 6499 of Proc. of SPIE, San Jose, California, USA, Jan 28 -Feb 1 2007.

[40] S. Gupta, M. P. Sampat, Z. Wang, M. K. Markey, and A. C. Bovik. 3d face recognition using the complex-wavelet structural similarity metric. In IEEE Workshop on Applications of Computer Vision, Austin, TX, 2007.

[41] K. I. Chang, K. W. Bowyer, and P. J. Flynn. Multimodal 2d and 3d biometrics for face recognition. In Analysis and Modeling of Faces and Gestures, 2003. AMFG 2003. IEEE International Workshop on, pages 187–194, 2003.

[42] A. Godil, S. Ressler, and P. Grother. Face recognition using 3d facial shape and color map information: comparison and combination. In Proceedings of the SPIE – The International Society for Optical Engineering, volume 5404, pages 351–361, Nat.Inst. of Stand. & Technol., Gaithersburg, MD, USA, 2004. SPIE-Int. Soc. Opt. Eng.

[43] M. Husken, M. Brauckmann, S. Gehlen, and C. Von der Malsburg. Strategies and benefits of fusion of 2d and 3d face recognition. In Computer Vision and Pattern Recognition, 2005 IEEE Computer Society Conference on, volume 3, pages 174–182, 2005.

[44] T. Maurer, D. Guigonis, I. Maslov, B. Pesenti, A. Tsaregorodtsev, D. West, and G. Medioni. Performance of geometrix activeidTM 3d face recognition engine on the frgc data. In Computer Vision and Pattern Recognition, 2005 IEEE Computer Society Conference on, volume 3, pages 154–161, 2005.

A Neural Network Based Diagnostic System for Classification of Industrial Carrying Jobs With Respect of Low and High Musculoskeletal Injury Risk

Rohit Sharma   r25sharma@gmail.com
Faculty of Engineering
Dayalbagh Educational Institute
Dayalbagh, Agra, 282110, India

Ranjit Singh   rsingh_dei@yahoo.com
Faculty of Engineering
Dayalbagh Educational Institute
Dayalbagh, Agra, 282110, India

Abstract

Even with many years of research efforts, Safety professionals and ergonomists have not yet been established the occupational exposure limits of different risk factors for development of Musculoskeletal disorders (MSDs). One of the main problems in setting such guidelines is to accurately assess the association between exposures and possible occupational disorders or diseases and predict the outcome of any variable. The task of an industrial ergonomist is complicated because the potential risk factors that may contribute to the onset of the MSDs interact in a complex way, and require an analyst to apply elaborate data measurement and collection techniques for a realistic job analysis. This makes it difficult to discriminate well between the jobs that place workers at high or low risk of MSDs. This paper describes a new approach for the development of artificial neural networks applied to classifying the risk of MSDs for industrial carrying jobs. The data set used in this research was collected from Foundry and Sugar industries workers using the physiological variables.The main objective of this study was to to develop an artificial neural network based diagnostic system which can classify industrial jobs according to the potential risk for physiological stressors due to workplace design. The neural network obtained can be used by the ergonomist as a diagnostic system, enabling jobs to be classified into two categories (low-risk and high-risk) according to the associated likelihood of causing MSDs. This system provides a higher proportion of correct classifications than other previous models. So, the system can be used as an expert system which, when properly trained, will classify carrying load by male and female industry workers into two categories of low risk and high risk work, based on the available characteristics factors.

Relevance to industry

A number of workers involve in lifting and carrying loads manually in industries. Such tasks may lead to various types of musculoskeletal injuries to the workers. So, this study was focussed on the development of an artificial neural network-based diagnostic system which can classify industrial jobs according to the low and high risk of MSDs. Such a system could be useful in hazard analysis and injury prevention due to manual handling of loads in industrial environments.

Keywords: Musculoskeletal Injuries, Physiological Risk, Artificial Neural Network

1. INTRODUCTION
Occupational health hazards are common in many sectors and are on the increase. Musculoskeletal disorders (MSDs), which are problems of musculoskeletal system, are significant and costly workplace problems affecting occupational health, productivity and the careers of the

working population. MSDs represent a wide range of disorders and are an important cause of morbidity and disability. At the present time, MSDs are one of the most important problems ergonomists encounter in Workplaces around the world [1]. In 2001, the National Institute for Occupation Safety and Health (NIOSH) defined musculoskeletal problems as a group of conditions that involved the nerves, tendons, muscles, and supporting structures such as inter vertebral discs. Studies from around the world have documented the enormous burden of musculoskeletal injuries on individuals and society [2]. These problems are caused by repetitive, awkward, or stressful motions, heavy lifting, frequent twisting and bending, whole body vibration, and psychosocial variables [3, 4, 5, 6, 7]

Work related neck and upper limb problems are very prevalent in nature. In the Netherlands, a survey showed that in 2002 and 2004, 28% of the working population reported neck/shoulder or elbow/wrist/hand symptoms in the previous 12 months. These symptoms were at least partly\caused by work, according to the self-report of the participants [8]. Yearly sick leave due to work related neck and upper limb problems are estimated to be 2 to 4% of all workers. Scutter et al. [9] reported that one third of agricultural workers surveyed reported neck pain at least once a week. Tractor driving was reported most frequently as the activity that contributed to neck pain. Low back pain (LBP) is also the most frequent musculoskeletal problem. Snook [10] estimated the annual direct and indirect costs of back pain to be almost $16 billion. The highest percent of such injuries occurred in service industries (31.9%), followed by manufacturing (29.4%), transportation and public utility (28.8%), and trade (28.4%). The total time lost due to disabling work injuries was 75 million work-days, with the total work accident cost of $47.1 billion, and the average cost per disabling injury of about $16,800. The economic impact of back injuries in the US alone may be as high as $20 billion annually. Nearly 2 million workers suffer from MSDs each year [11].The economic loss due to such disorders affects not only the individual but also the organization and the society as whole [12]. In industrially developing countries (IDCs) the problems of workplace injuries are extremely serious [13]. In many countries the prevention of MSDs among the workforce is considered a national priority [14].

2. METHODOLOGY

2.1   Artificial Neural Network
In neural computing, mathematical processing units (neurons) are linked together by weighted connections. Each neuron processes its weighted inputs according to its activation function, and its output is then connected to the inputs of the next layer of neurons. Networks usually have a non-linear activation function, of which a popular choice is the logistic (sigmoidal) activation function. By allocating appropriate values to the weights, an Artificial Neural Network (ANN) can perform complicated operations on its inputs. A network can be trained to perform a particular operation using a set of training data comprising a series of input patterns for which the correct output is known. Each training pattern is presented to-the inputs in turn. The network weights, originally set to random values, are then optimized using a training algorithm. Training continues until the errors associated with the training set are minimized. Neural networks can solve classification problems when the input data is difficult to describe, and therefore hold promise for medical applications [15].

2.2   ANN Architecture
In this study, a feedforward neural network with error back-propagation training was implemented [16, 17]. During supervised error-back propagation training, input patterns are presented sequentially to the system along with the correct response. The response is provided by the teacher and specifies the classification information for each input pattern. The network learns from experience by comparing the targeted correct response with the actual response. The network parameters (weights and thresholds) are usually adjusted after each incorrect response based on the error value generated. This process of comparison of correct and actual response is continued for each input pattern until all examples from the training set are learned within an acceptable error. During the classification phase, the trained neural network itself operates in a

feedforward manner. The input pattern is passed forward through the network one layer at a time from the input to the output, with no feedback. The network should be able to classify accurately in situations not encountered in training. The architecture of an ANN model is shown in figure 1.
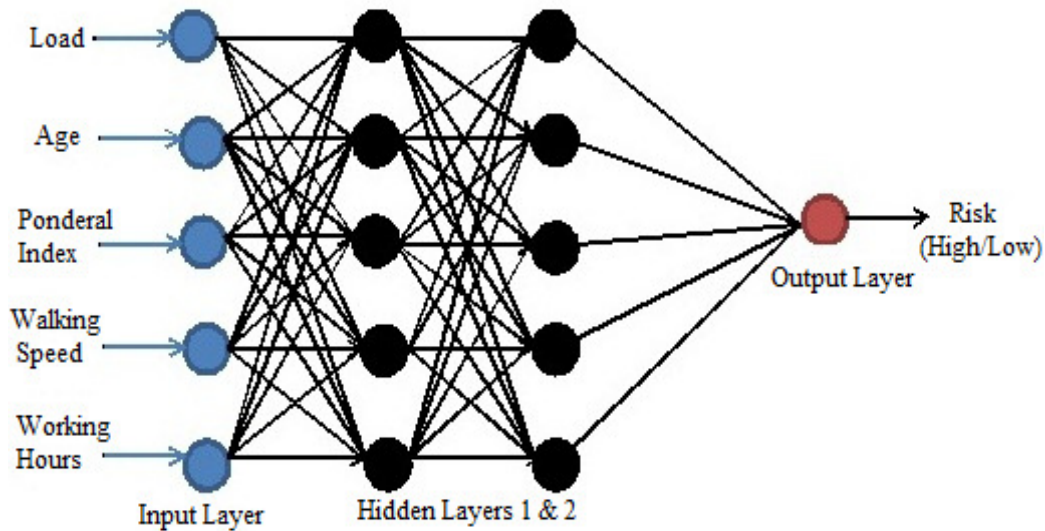

FIGURE 1: The Architecture of the proposed artificial neural network model.

The task of the industrial ergonomist is fairly difficult because the potential risk factors that may contribute to the MSDs in a complex way, and require him or her to apply elaborate data measurement and collection techniques for a realistic job analysis. If an Expert System is made, which can classify the loads carried in different categories of risk, than the potential risks involved can be avoided. Hence, a Neural Network Model which will act as a knowledge base system for the classification of carried load in different risk categories will be of great use. Some researchers also found the successful implementation of the ANN in classifying manual lifting jobs. Karwowski et al. [18] presented a prototype of a neural network-based system for classification of industrial jobs according to the potential risk for LBDs. Although the system was trained using a limited number of data for 60 high and low risk jobs the preliminary results showed that the developed diagnostic system could successfully classify jobs into the low and high risk categories of LBDs based on lifting task characteristics. The jobs were correctly classified into the low and high risk categories in about 80% of cases. Zurada [19] also found that a developed diagnostic system can successfully classify jobs into the low and high risk categories of LBDs based on lifting task characteristics. So, the main objective of this study was to develop an artificial neural network based diagnostic system which can classify industrial jobs according to the potential risk for physiological stressors due to workplace design. Such a system could be useful in hazard analysis and injury prevention due to manual handling of loads in industrial environments.

2.3 Experimental Data for Model Development

This study involved an acceptable load for male and female workers involved in carrying load in high and low risk work. Since the preference of the workers was in head mode so the data taken for training neural network was for head mode only. For training neural network, the data from specially prepared questionnaire and experimental in laboratory of the male and female workers involved in Foundry and Sugar industries were used. Their physiological stress were divided into two groups, high and low risk work based upon the factors load carried, age, ponderal index, walking speed and working hours as the increase or decrease in the values of these factors influence the physiological stress. These factors were applied as the input during network's training and testing. Physiological stress and heart beats per minute records were used to categorize high and low risk work. The low risk and high risk work was defined as those jobs or load carried by male and female workers with physiological stress and heart rate depending upon age with ponderal index, working hour and walking speed.

Mathematically we summarize this as,

$$Y = f\left(\text{L, A, PI, WS, WH}\right) \qquad\qquad .... (1)$$

Where,

Y = .1 < Physiological risk factor < .9
L= 8 < Load <51 Kg
A = 21 < Age < 52 years
PI = 23 < Ponderal index < 26.2
WS = 2 < Walking Speed < 3.9 km/hr
WH = 5 < Working Hours < 8 hrs.

2.4   Normalization of Training Data

The values of the input variables for male and female workers are given in table1 and 2. To prevent network's saturation [19], these variables were normalized in between [0.1 0.9] by a programme written in Matlab. The Y variable (risk of load carrying) takes values of 0.9 or 0.1 for high and low risk work, respectively. This variable was used only as teacher's response during the network's training using error back propagation algorithm.

2.5   Network Training and Development of Model

The network was trained in MATLAB environment software programmed by exploiting Neural Network Toolbox model version R.2010.a. This software is chosen due to its capabilities and ability to provide solutions in technical computing. Among various training algorithm available, Levenberg-Marquardt (LM) training function was selected because it has the fastest convergence ability [20]. Out of the 72 sets of observations with low and high risk values recorded for male workers 65 sets were used for training and development of model and in case of female workers out of 66 sets of observations with low and high physiological risk 56 sets were used for training of the ANN.

2.6   MAT LAB Programme for Development of ANN Model

```
clc;
clear all;
close all;
x=data
x=[normal1(x(:,1)) normal1(x(:,2)) normal1(x(:,3)) normal1(x(:,4)) normal1(x(:,5)) normal1(x(:,6))];
t=x(1:65,6);p=x(1:65,1:5);
 p=p';t=t';
net=newff(minmax(p),[5,5,1],{'tansig','tansig','purelin'});
net.trainParam.show = 20;
net.trainParam.epochs = 3000;
net.trainParam.goal = 1e-8;
[net,tr]=train(net,p,t);
p=x(1:72,1:5);p=p';d=x(1:72,6);
 y=sim(net,p);y=y';
 k=[y d];p=p';
plot(k)
figure(2)
k1=[p(:,1) y];
plot(k1)
figure(3)
k2=[p(:,2) y];
plot(k2)
figure(4)
k3=[p(:,3) y];
plot(k3)
figure(5)
```

```
k4=[p(:,4) y];
plot(k4)
figure(6)
k5=[p(:,5) y];
plot(k5)
```
Above Mat lab code include file of data which refers to male and female workers observations sets given in table 1 and 2.

Test run of Model
After the training of the network the model so trained and developed is tested for all sets of observation in case of male (72) and female workers (66).

3. RESULTS AND DISCUSSION

3.1 Simulation Results- Male Workers

FIGURE 2: Training error versus number of training cycles (Epochs)

FIGURE 3: Output of trained ANN network

FIGURE 4: Comparison of output of trained ANN network and 1st input

FIGURE 5: Comparison of output of trained ANN network and 2nd input

FIGURE 6: Comparison of output of trained ANN network and 3rd input

Rohit Sharma & Ranjit Singh

FIGURE 7: Comparison of output of trained ANN network and 4th input
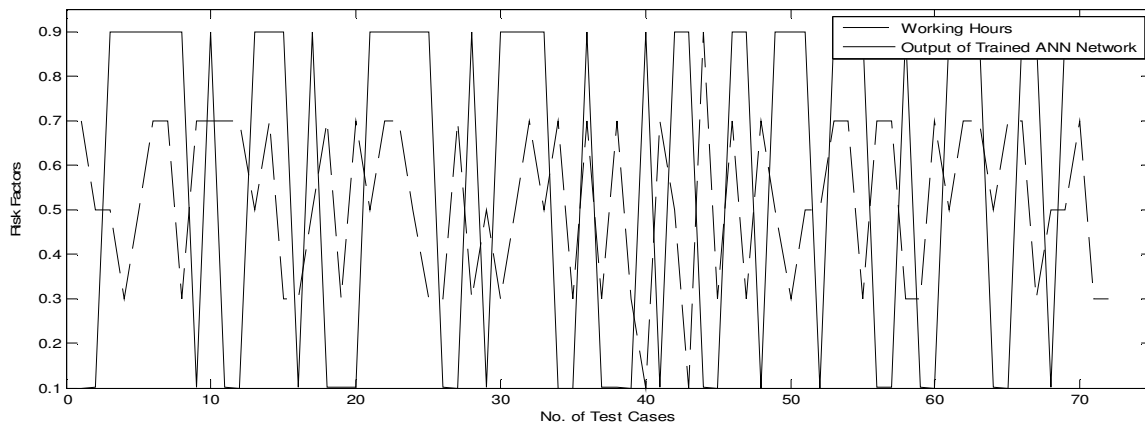
FIGURE 8: Comparison of output of trained ANN network and 5th input

Figure 2 shows the training of the neural network for the first 65 sets of observation of the male workers and figure 3 shows the output of the trained neural network in the interval of [0.1 0.9]. Figures 4 to 8 show the plotting of trained neural model for all the sets of observations with the inputs of the ANN and the figures showed that as the magnitude of load, age, walking speed and working hours of these factors increases, the risk increases.

3.2 Simulation Results – Female Workers
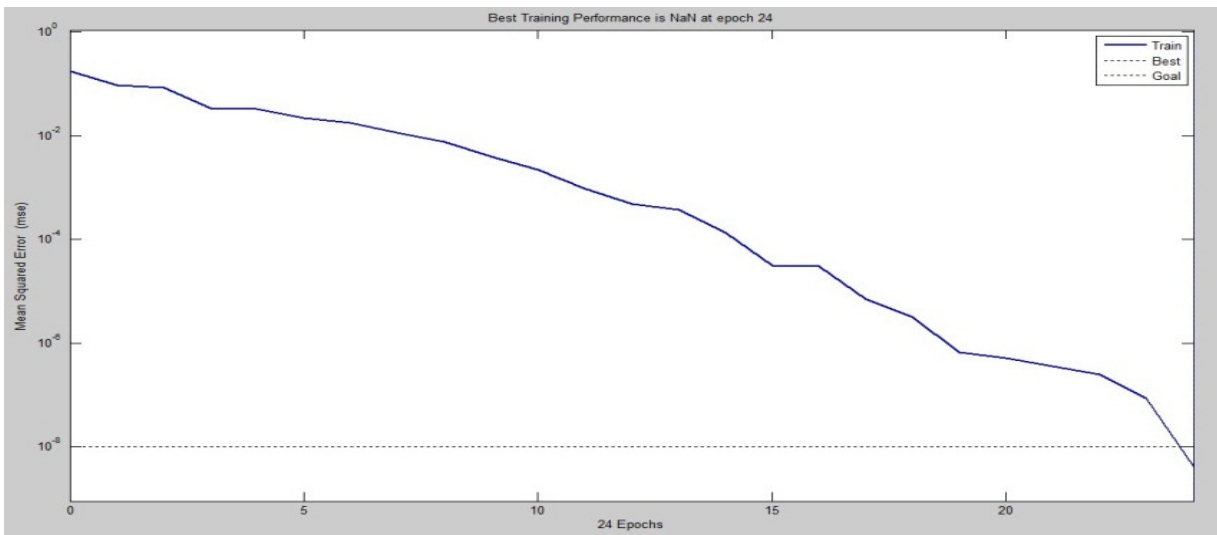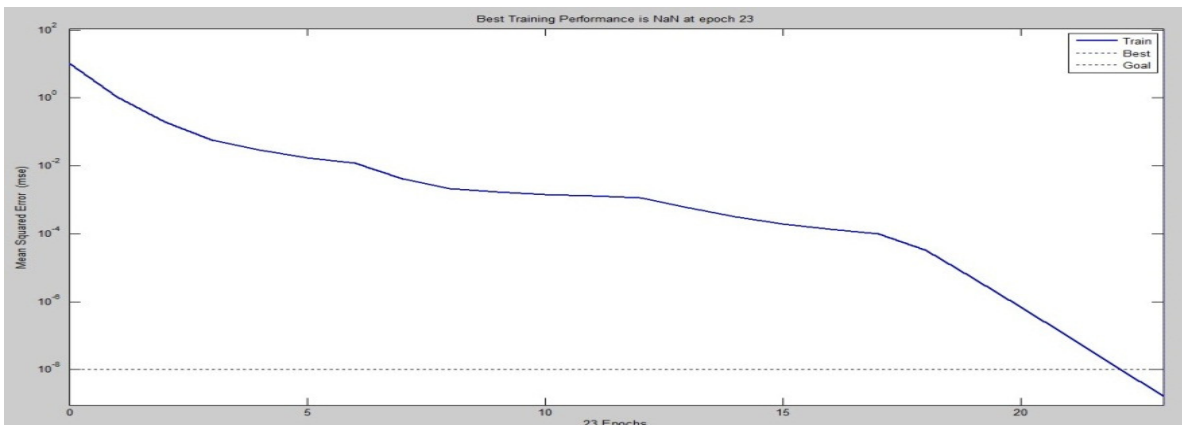

FIGURE 9: Training error versus number of training cycles (Epochs)
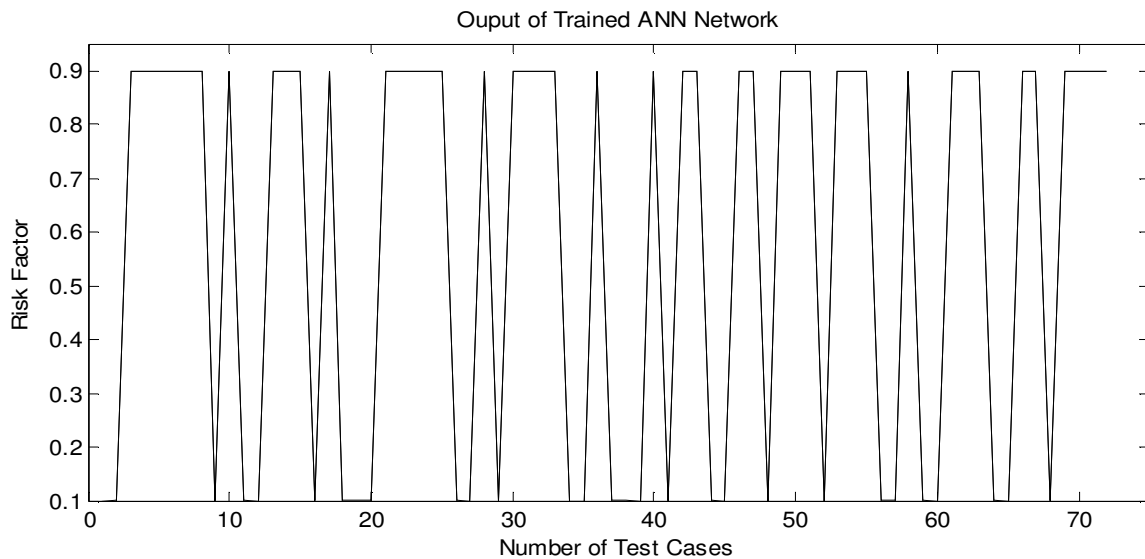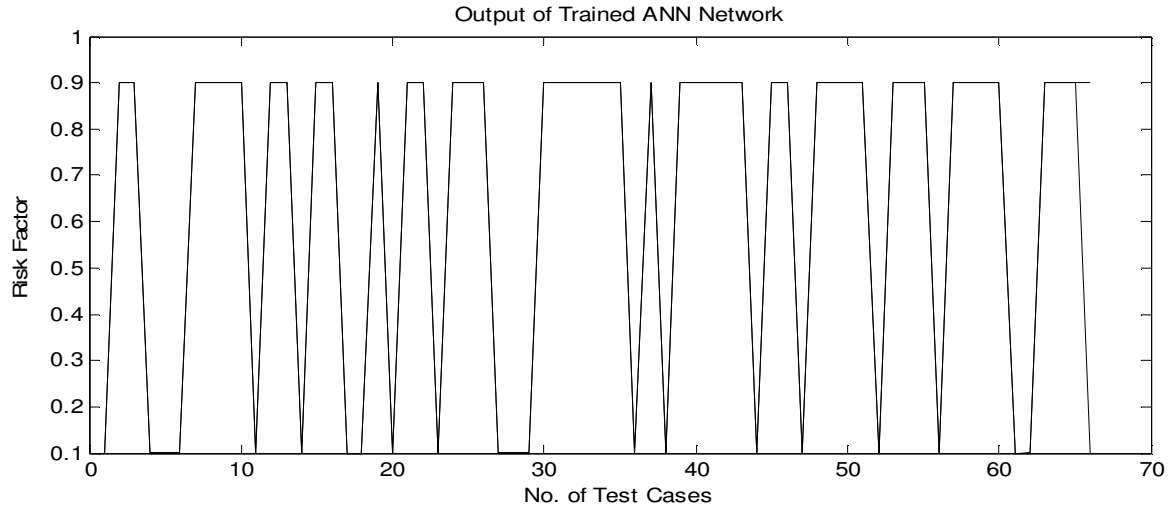
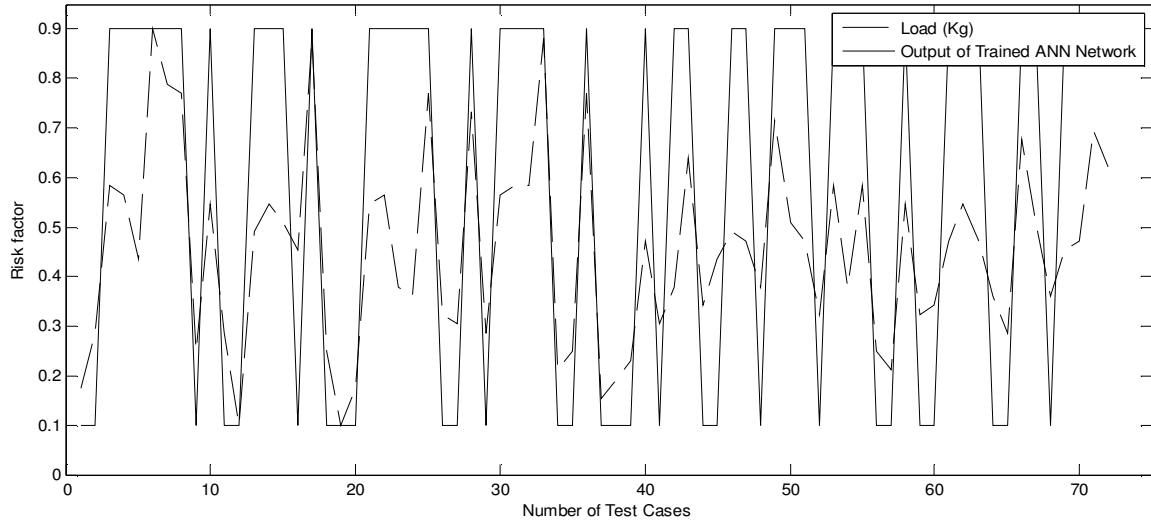**FIGURE 10**: Output of trained ANN network
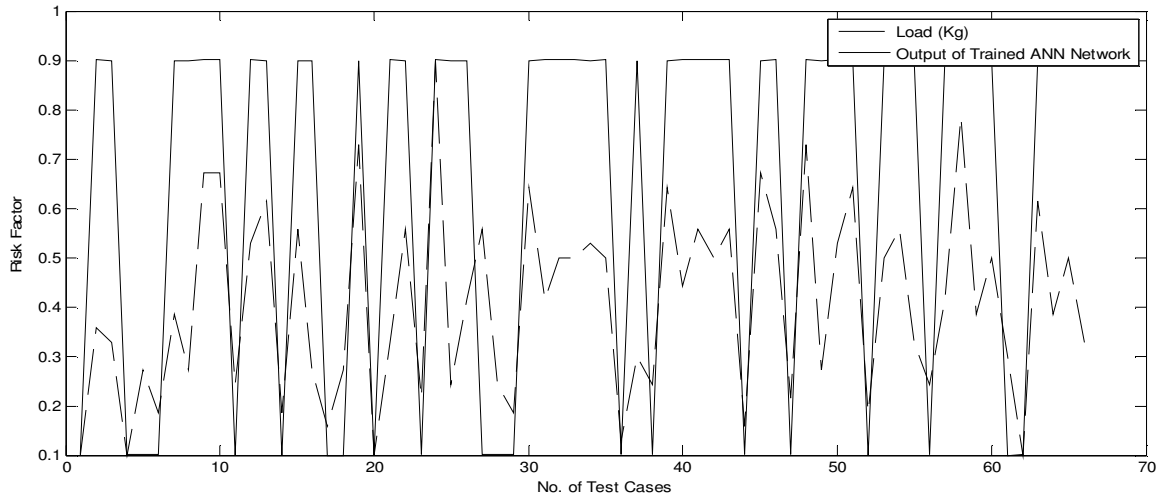
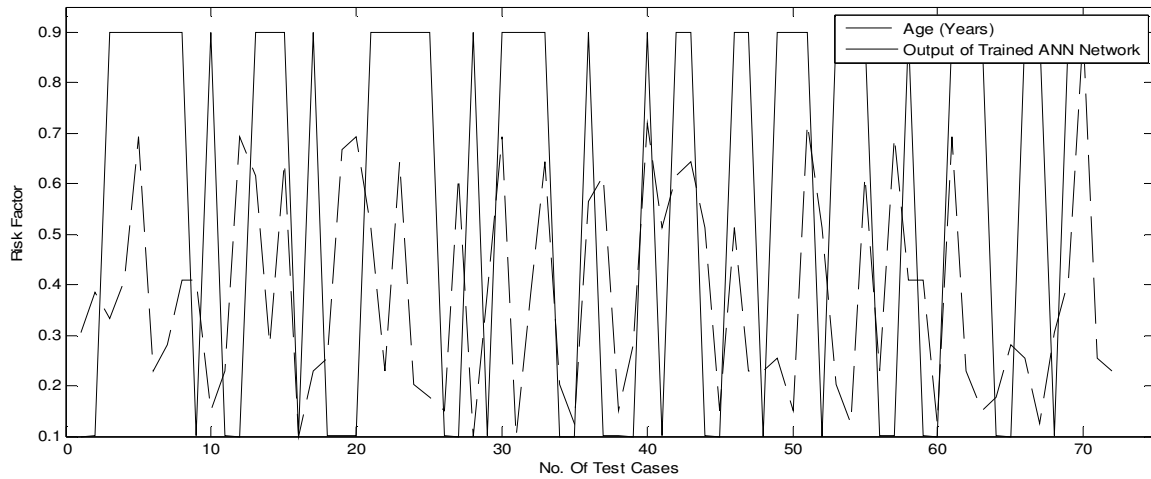**FIGURE 11:** Comparison of output of trained ANN network and 1st input
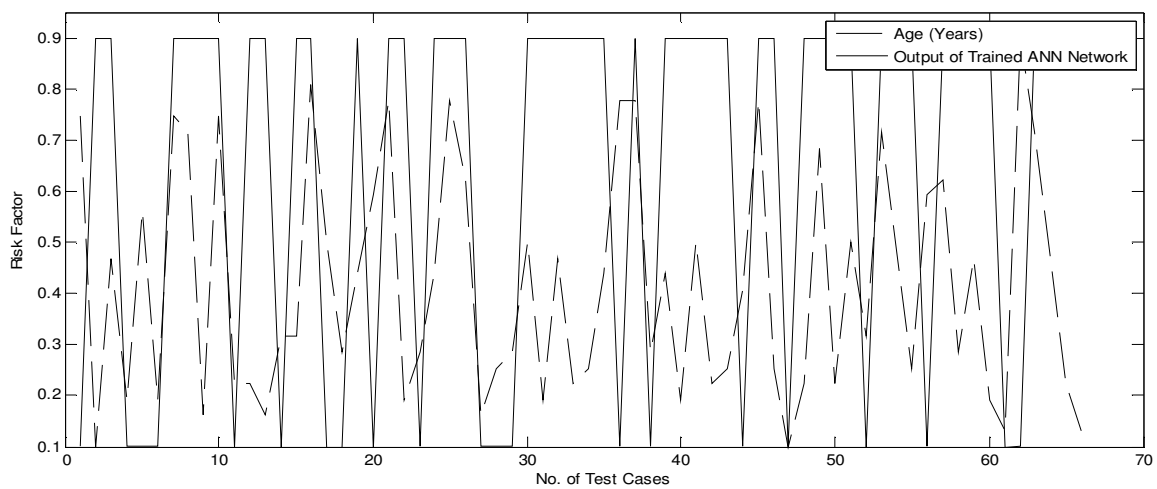
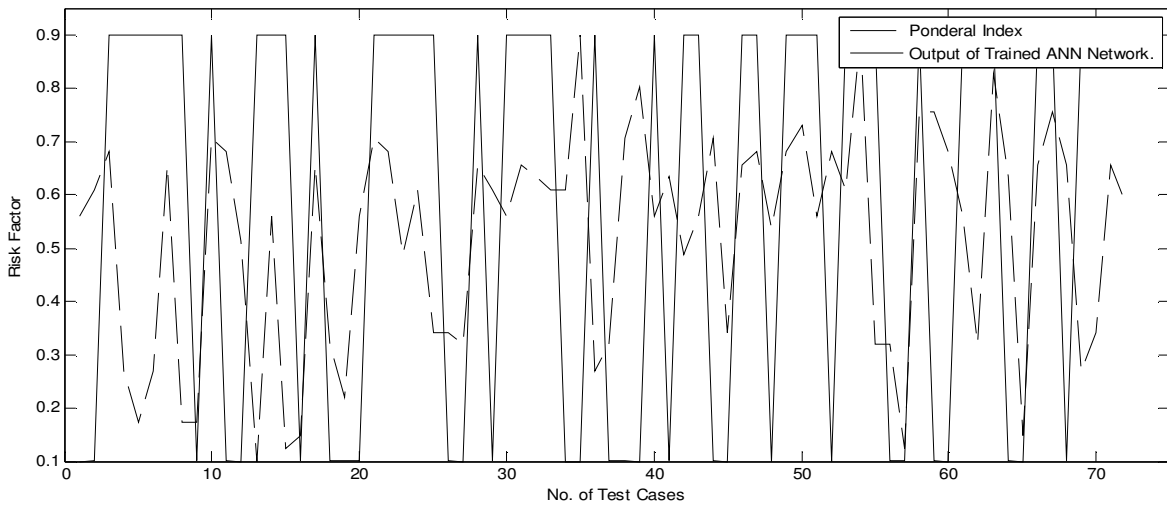**FIGURE 12:** Comparison of output of trained ANN network and 2nd input

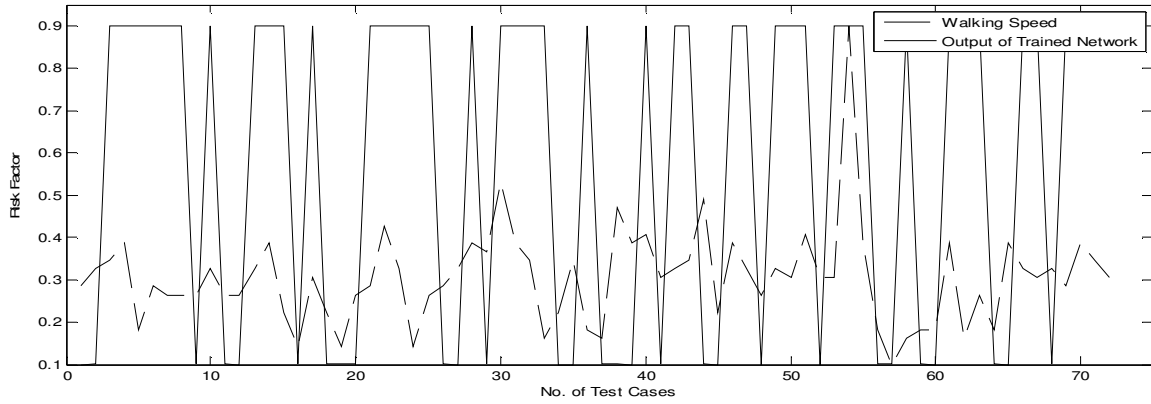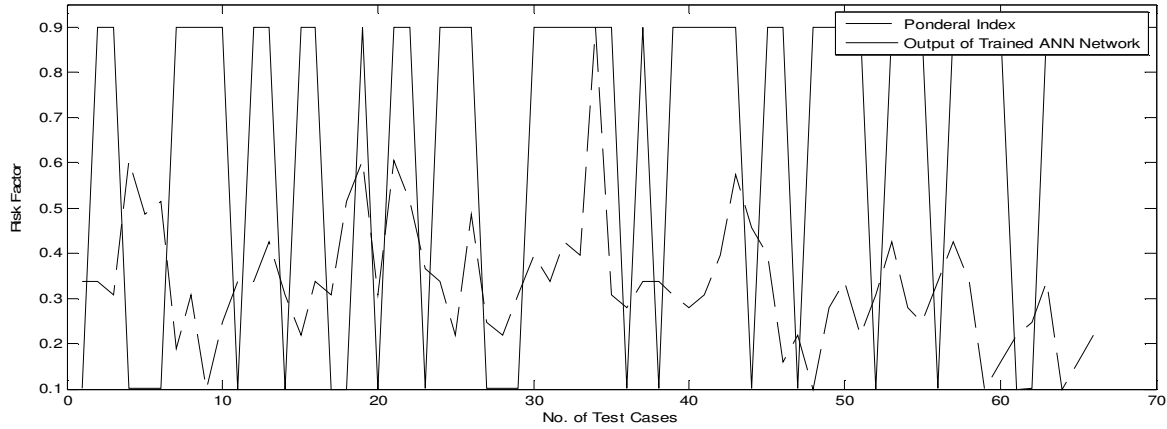**FIGURE 13:** Comparison of output of trained ANN network and 3rd input
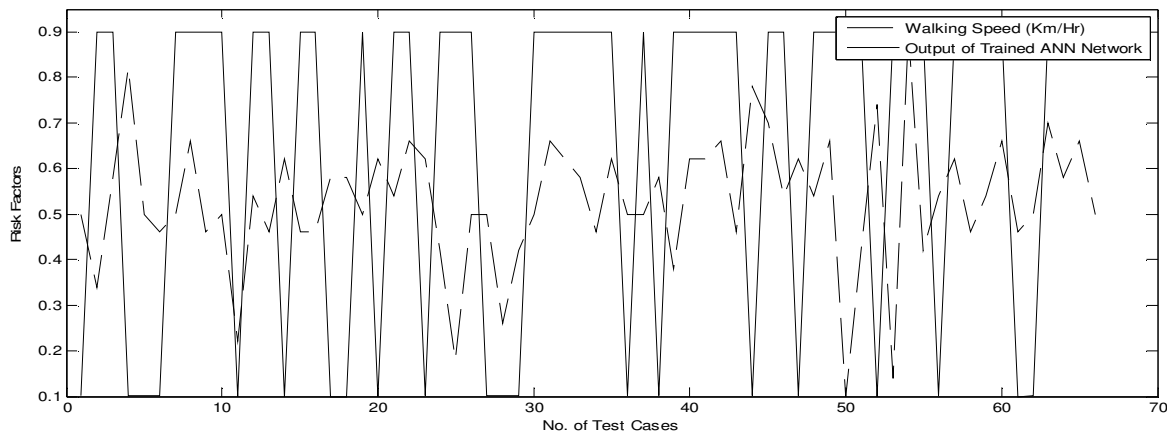
FIGURE 14: Comparison of output of trained ANN network and 4th input
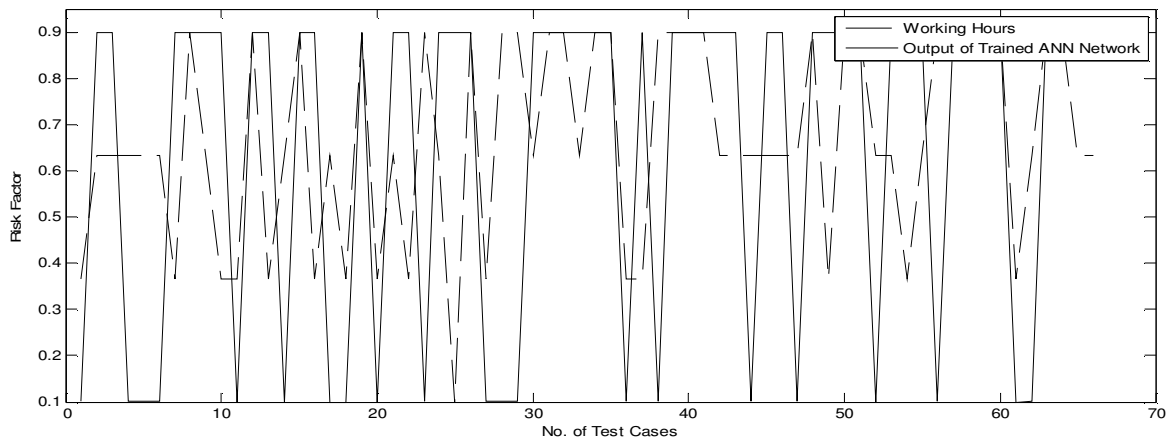
FIGURE 15: Comparison of output of trained ANN network and 5th input

Figure 9 shows the training of the neural network for the first 56 sets of observation of the female workers and figure 10 shows the output of the trained neural network in the interval of [0.1 0.9]. Figures 11 to 15 show the plots of trained neural model for all the sets of observations with the inputs of the ANN and show that as the magnitude of load, age, walking speed and working hours of these factors increases or decreases, the risk also increases or decreases.

TABLE 1: The percentage variation in experimental and simulated results (Male workers)

S.No.	Load (kg)	Age (year)	Ponderal Index	Walking Speed	Working Hours	Risk		Percentage variation (%)
						Physiological	ANN Simulation	
1.	12	29	24.8	2.7	8	Low	Low	0.014517
2.	18	32	25	2.9	7	Low	Low	0.006739
3.	34	30	25.3	3	7	High	High	0.000349
4.	33	33	23.6	3.2	6	High	High	-0.00087
5.	26	44	23.2	2.2	7	High	High	-0.00753
6.	51	26	23.6	2.7	8	High	High	0.002771
7.	45	28	25.2	2.6	8	High	High	0.006082
8.	44	33	23.2	2.6	6	High	High	0.002217
9.	16	33	23.2	2.6	8	Low	Low	0.289529
10.	32	23	25.4	2.9	8	High	High	0.002228
11.	18	26	25.3	2.6	8	Low	Low	0.0421
12.	8	44	24.6	2.6	8	Low	Low	0.019635
13.	29	41	22.9	2.9	7	High	High	-0.00398
14.	32	28	24.8	3.2	8	High	High	-0.00056
15.	30	42	23	2.4	6	High	High	-0.00216
16.	27	21	23.1	2	6	Low	Low	0.000605
17.	50	26	25.2	2.8	7	High	High	0.003725
18.	16	27	23.8	2.4	8	Low	Low	0.043644
19.	8	43	23.4	2	6	Low	Low	0.029657
20.	12	44	24.8	2.6	8	Low	Low	0.006035
21.	32	37	25.4	2.7	7	High	High	-0.00055
22.	33	26	25.3	3.4	8	High	High	0.000216
23.	23	42	24.5	2.9	8	High	High	-0.02341
24.	22	25	25	2	7	High	High	-0.02488
25.	44	24	23.9	2.6	6	High	High	0.001041
26.	20	23	23.9	2.7	6	Low	Low	-0.15115
27.	19	41	23.8	2.9	8	Low	Low	-0.21189
28.	42	21	25.2	3.2	6	High	High	-0.0024
29.	18	32	25	3.1	7	Low	Low	0.005013
30.	33	44	24.8	3.9	6	High	High	-0.00117
31.	34	21	25.2	3.2	7	High	High	0.010481
32.	34	32	25.1	3	8	High	High	0.000466
33.	50	42	25	2.1	7	High	High	0.003174
34.	14	25	25	2.4	8	Low	Low	0.042572
35.	16	22	26.2	3	6	Low	Low	0.00782
36.	44	39	23.6	2.2	8	High	High	0.00255
37.	11	41	23.8	2.1	6	Low	Low	0.006824
38.	13	23	25.4	3.6	8	Low	Low	-0.21649
39.	15	28	25.8	3.2	6	Low	Low	0.004896
40.	28	45	24.8	3.3	5	High	High	-0.01014
41.	19	37	25.1	2.8	8	Low	Low	0.033211
42.	23	41	24.5	2.9	7	High	High	0.005072
43.	37	42	24.8	3	5	High	High	0.000906
44.	21	37	25.4	3.7	9	Low	Low	-0.01588
45.	26	23	23.9	2.4	6	Low	Low	0.001795
46.	29	37	25.2	3.2	8	High	High	-0.00503
47.	28	26	25.3	2.9	6	High	High	0.002094
48.	23	26	24.7	2.6	8	Low	Low	-0.25723

49.	41	27	25.3	2.9	7	High	High	0.002542
50.	30	23	25.5	2.8	6	High	High	0.022776
51.	28	45	24.8	3.3	7	High	High	-0.00756
52.	20	37	25.3	2.8	7	Low	Low	0.086335
53.	34	25	25	2.8	8	High	High	0.001987
54.	23	22	26.2	5.7	8	High	High	0.003125
55.	34	41	23.8	3.2	6	High	High	-0.00051
56.	16	26	23.8	2.2	8	Low	Low	0.124038
57.	14	44	23	1.8	8	Low	Low	-0.11788
58.	32	33	25.6	2.1	6	High	High	0.000293
59.	20	33	25.6	2.2	6	Low	Low	-0.36982
60.	21	22	25.3	2.2	8	Low	Low	-0.06034
61.	28	44	24.8	3.2	7	High	High	-0.00712
62.	32	26	23.8	2.1	8	High	High	0.000925
63.	28	23	25.9	2.6	8	High	High	0.000795
64.	22	24	25.1	2.2	7	Low	Low	-0.03006
65.	18	28	23.1	3.2	8	Low	Low	-0.00894
66.	39	27	25.2	2.9	8	High	High	0.003506
67.	30	22	25.6	2.8	6	High	High	0.101124
68.	22	29	25.2	2.9	7	Low	Low	1.025248
69.	27	33	23.6	2.7	7	High	High	-0.00596
70.	28	52	23.9	3.2	8	High	High	-0.00727
71.	40	27	25.2	3	6	High	High	0.001816
72.	36	26	24.9	2.8	6	High	High	0.000844

TABLE 2: The percentage variation in experimental and simulated results (Female workers)

S.No.	Load (kg)	Age (year)	Ponderal Index	Walking Speed	Working Hours	Risk		Percentage variation (%)
						Physiological	ANN Simulation	
1.	12	42	23.2	2.8	6	Low	Low	0.01732
2.	21	21	23.2	2.4	7	High	High	0.015001
3.	20	33	23.1	3	7	High	High	0.009011
4.	12	24	24.1	3.6	7	Low	Low	-0.04509
5.	18	36	23.7	2.8	7	Low	Low	-0.19893
6.	15	24	23.8	2.7	7	Low	Low	0.064624
7.	22	42	22.7	2.8	6	High	High	0.001357
8.	18	41	23.1	3.2	8	High	High	0.023939
9.	32	23	22.4	2.7	7	High	High	0.001186
10.	32	42	22.9	2.8	6	High	High	0.004302
11.	17	25	23.2	2.1	6	Low	Low	0.06396
12.	27	25	23.2	2.9	8	High	High	-0.00896
13.	30	23	23.5	2.7	6	High	High	0.000986
14.	15	28	23.1	3.1	7	Low	Low	0.012451
15.	28	28	22.8	2.7	8	High	High	-0.00821
16.	18	44	23.2	2.7	6	High	High	-0.00098
17.	14	34	23.1	3	7	Low	Low	0.057785
18.	18	27	23.8	3	6	Low	Low	0.077637
19.	34	32	24.1	2.8	8	High	High	-0.01928
20.	12	37	23.1	3.1	6	Low	Low	0.004904
21.	20	43	24.1	2.9	7	High	High	0.014895
22.	28	24	23.8	3.2	6	High	High	0.000232

23.	16	27	23.3	3.1	8	Low	Low	0.009932
24.	40	32	23.2	2.6	7	High	High	-0.01064
25.	17	43	22.8	2	5	High	High	-0.00042
26.	23	38	23.7	2.8	8	High	High	-0.01407
27.	28	23	22.9	2.8	6	Low	Low	0.006109
28.	17	26	22.8	2.2	8	Low	Low	0.010578
29.	15	27	23.1	2.6	8	Low	Low	0.007079
30.	31	34	23.4	2.8	7	High	High	-0.00805
31.	23	24	23.2	3.2	8	High	High	0.02017
32.	26	33	23.5	3.1	8	High	High	-0.0127
33.	26	25	23.4	3	7	High	High	0.028119
34.	27	26	25.1	2.7	8	High	High	9.01E-06
35.	26	32	23.1	3.1	8	High	High	-0.01147
36.	13	43	23	2.8	6	Low	Low	-0.03634
37.	19	43	23.2	2.8	6	High	High	-0.00078
38.	17	27	23.2	3	8	Low	Low	0.002666
39.	31	32	23.1	2.5	8	High	High	-0.01008
40.	24	24	23	3.1	8	High	High	0.004068
41.	28	34	23.1	3.1	8	High	High	-0.01198
42.	26	25	23.4	3.2	7	High	High	-0.00291
43.	28	26	24	2.7	7	High	High	7.06E-05
44.	14	31	23.6	3.5	7	Low	Low	0.158553
45.	32	43	23.4	3.3	7	High	High	-0.01279
46.	28	26	22.6	2.9	7	High	High	-0.00345
47.	16	21	22.8	3.1	7	Low	Low	0.009754
48.	34	25	22.4	2.9	8	High	High	-0.00569
49.	18	40	23	3.2	6	High	High	-0.00407
50.	27	25	23.2	1.8	8	High	High	0.016232
51.	31	34	22.8	2.6	8	High	High	-0.01043
52.	15	28	23.1	3.4	7	Low	Low	-0.01214
53.	26	41	23.5	1.9	7	High	High	0.00024
54.	28	33	23	3.8	6	High	High	-0.01196
55.	20	26	22.9	2.6	7	High	High	0.030324
56.	17	37	23.2	2.9	8	Low	Low	-0.16531
57.	23	38	23.5	3.1	8	High	High	-0.0135
58.	36	27	23.2	2.7	8	High	High	-0.00911
59.	22	33	22.4	2.9	8	High	High	-0.00933
60.	26	24	22.6	3.2	8	High	High	-0.00599
61.	19	22	22.8	2.7	6	Low	High	-799.415
62.	12	47	22.9	2.8	7	Low	Low	0.095916
63.	30	41	23.2	3.3	8	High	High	-0.01307
64.	22	33	22.4	3	8	High	High	-0.00999
65.	26	25	22.6	3.2	7	High	High	-0.00702
66.	20	22	22.8	2.8	7	Low	High	-784.575

Neural Network model developed in this study can predict physiological stress in the male and female workers involved in Foundry and Sugar industry based on five input parameters. The results obtained using LM training for back propagation NN give good prediction and are validated with experimental values as indicated in Table 1 and 2. These results suggest that ANN is a powerful tool for predictive application. ANN captures the intricate relationship among various process parameters and can be integrated readily into an existing environment. Table 3 shows a comparison between results of past studies models and the current study model in terms of accuracy in classifying physiological stress in Low and High risk and the current study has an

edge over the past studies, as it provides a higher proportion of correct classifications (97%) than other previous models.

TABLE 3: Comparison of the results of previous studies and current approach.

Zurada et. al., 1997	Asensio-Cuesta et. al. 2010	Current Study
industrial jobs for LBDs about 75%	Highly repetitive lifting industrial jobs for LBDs about 87%	Industrial carrying jobs for MSDs about 97%

4. CONCLUSION

The results of this study show that an artificial neural network-based diagnostic system can be used as an expert system which, when properly trained, will allow us to classify carrying loads by male and female workers into two categories of low and high risk work, based on the available characteristics factors. The developed neural network based classification system shows great promise because it identifies and classifies industrial jobs into the high and low risk potential for physiological risk and significantly reduces the time consuming job analysis and classification performed by traditional methods like mathematical modeling. Finally this technique open new overseas of parameters estimation, function approximation, optimization and online control of the complex system. Future work will focus on validation of the ANN architecture, and consider utilization of other input variables for the modeling, including individual characteristics of the workers, and the job stressors such as job satisfaction, work autonomy, workload, and other psychosocial parameters.

5. REFERENCES

[1] H. Demuth and M. Beale, "Neural network toolbox for use with MATLAB," user guide version 4. The MathWorks, Inc. USA, 2004.

[2] J.W. Frank, M.S. Kerr, A.S. Brooker, S.E. DeMaio, A. Maetzel, H.S. Shannon, T.J. Sullivan and R.W. Norman. R.P. Wells. Disability resulting from occupational low back pain. Part I: What do we know about primary prevention? A review of the scientific evidence on prevention before disability begins. Spine, 1996, vol. 21, pp. 2908–2917.

[3] A. Burdorf and G. Sorock. "Positive and negative evidence of risk factors for back disorders," Scand J Work Environ Health, 1997, vol. 23, pp. 243–256.

[4] W.E. Hoogendoorn, M.N. van Poppel, P.M. Bongers, B.W. Koes and L.M. Bouter. "Physical load during work and leisure time as risk factors for backpain," Scand J Work Environ Health, 1999, vol. 25, pp. 387–403.

[5] W.E. Hoogendoorn, M.N. van Poppel, P.M. Bongers, B.W. Koes and L.M. Bouter. "Systematic review of psychosocial factors at work and private life as risk factors for back pain," Spine, 2000, vol. 25, pp. 2114–2125.

[6] M. Lagerstrom, T. Hansson and M. Hagberg. "Work-related low-back problems in nursing," Scand J Work Environ Health, 1998, vol. 24, pp. 449–464.

[7] K. Vanwonterghem. "Work-related musculoskeletal problems: some ergonomics consideration," J Hum Ergol, 1996, vol. 25, pp. 5-13.

[8] J. Heinrich and B.M. Blatter. RSI symptoms in the Dutch labour force. Trends, risk factors and explanations. TSG, 2005, vol. 83, pp.16–24.

[9] S. Scutter, D.S. Turker and R. Hall. "Headaches and neck pain in farmers," Australian Journal of Rural Health, 1997, vol. 5, no. 1, pp. 2-5.

[10] S. H. Snook. "The Costs of Back Pain in Industry," Occupational Medicine: State-of-the-Art Reviews, 1988, vol. 3, no. 1, pp. 1-50.

[11] S. Laderas, A.L. Felsenfeld. "Ergonomics and the dental office: an overview and consideration of regulatory influences" J Calif Dent Assoc, 2002, vol. 30, no. 2, pp.7-8.

[12] K. Kemmlert. "Labor inspectorate investigation for the prevention of occupational musculoskeletal injuries," (licentiate thesis) Solna, Sweden: National Institute of Occupational Health, 1994.

[13] H. Shahnavaz. "Workplace injuries in the developing countries," Ergonomics, 1987, vol. 30, pp. 397-404.

[14] P. Spielholz, B. Silverstein, M. Morgan, H. Checkoway, and J. Kaufman. "Comparison of self-report, video observation and direct measurement methods for upper extremity musculoskeletal disorder physical risk factors," Ergonomics, 2001, vol. 44, pp. 588-613.

[15] J. Allen, and A. Murray. "Development of a neural network screening aid for diagnosing lower limb peripheral vascular disease from photoelectric plethysmography pulse waveforms," Physiol. Meas., 1993, vol. 14, pp. 13-22.

[16] I.W. Habib. "Neuro computing in high-speed network," IEEE Communications Magazine October, 1995, pp. 38-40.

[17] J. M. Zurada. "Introduction to Artificial Neural Systems," West Publishing, St. Paul, Minnesota, 1992.

[18] W. Karwowski, J. Zurada, W.S. Marras and P. Gaddie. "A prototype of the artificial neural network-based system for classification of industrial jobs with respect to risk of low back disorders in Aghazadeh," F. (ed) proceedings of the Industrial Ergonomics & Safety Conference, Taylor & Francis, London, 1994, pp. 19-22.

[19] J. Zurada, W. Karwowski and W. S. Marras. "A neural network-based system for classification of industrial jobs with respect to risk of low back disorders due to workplace design," Applied Ergonomics, Elsevier, 1997, Vol. 28, No. 1, pp. 49-58.

[20] More, J. J. "The Levenberg - Maquardt Algorithm: Implementation and theory, Numerical Analysis," G. A. Watson (Ed.), Lecture Notes in Mathematics, Springer Verlag, 1977, Vol. 630, pp.105-116.

[21] S. Asensio-Cuesta, J.A. Diego-Mas, J. Alcaide-Marzal. "Applying generalized feedforward neural networks to classifying industrial jobs in terms of risk of low back disorders," International journal of Industrial Ergonomics, 2010, Vol. 40, pp. 629-635.

INSTRUCTIONS TO CONTRIBUTORS

The *International Journal of Biometric and Bioinformatics (IJBB)* brings together both of these aspects of biology and creates a platform for exploration and progress of these, relatively new disciplines by facilitating the exchange of information in the fields of computational molecular biology and post-genome bioinformatics and the role of statistics and mathematics in the biological sciences. Bioinformatics and Biometrics are expected to have a substantial impact on the scientific, engineering and economic development of the world. Together they are a comprehensive application of mathematics, statistics, science and computer science with an aim to understand living systems.

We invite specialists, researchers and scientists from the fields of biology, computer science, mathematics, statistics, physics and such related sciences to share their understanding and contributions towards scientific applications that set scientific or policy objectives, motivate method development and demonstrate the operation of new methods in the fields of Biometrics and Bioinformatics.

To build its International reputation, we are disseminating the publication information through Google Books, Google Scholar, Directory of Open Access Journals (DOAJ), Open J Gate, ScientificCommons, Docstoc and many more. Our International Editors are working on establishing ISI listing and a good impact factor for IJBB.

The initial efforts helped to shape the editorial policy and to sharpen the focus of the journal. Starting with volume 6, 2012, IJBB appears in more focused issues. Besides normal publications, IJBB intend to organized special issues on more focused topics. Each special issue will have a designated editor (editors) – either member of the editorial board or another recognized specialist in the respective field.

We are open to contributions, proposals for any topic as well as for editors and reviewers. We understand that it is through the effort of volunteers that CSC Journals continues to grow and flourish.

LIST OF TOPICS
The realm of International Journal of Biometrics and Bioinformatics (IJBB) extends, but not limited, to the following:

- Bio-grid
- Bioinformatic databases
- Biomedical image processing (registration)
- Biomedical modelling and computer simulation
- Computational intelligence
- Computational structural biology
- DNA assembly, clustering, and mapping
- Fuzzy logic
- Gene identification and annotation
- Hidden Markov models
- Molecular evolution and phylogeny
- Molecular sequence analysis

- Bio-ontology and data mining
- Biomedical image processing (fusion)
- Biomedical image processing (segmentation)
- Computational genomics
- Computational proteomics
- Data visualisation
- E-health
- Gene expression and microarrays
- Genetic algorithms
- High performance computing
- Molecular modelling and simulation
- Neural networks

CALL FOR PAPERS

Volume: 6 - **Issue:** 3 - June 2012

i. Paper Submission: March 31, 2012   **ii. Author Notification:** May 15, 2012

iii. Issue Publication: June 2012

CONTACT INFORMATION